Bio-Design and Manufacturing (2021) 4:258–277
https://doi.org/10.1007/s42242-020-00104-5

REVIEW

Biofabrication of aligned structures that guide cell orientation and applications in tissue engineering

Kejie Lu[1] · Ying Qian[1] · Jiaxing Gong[1] · Ziyu Zhu[1] · Jun Yin[2] · Liang Ma[2] · Mengfei Yu[1] · Huiming Wang[1]

Received: 9 July 2020 / Accepted: 15 October 2020 / Published online: 22 January 2021

Abstract

The organized alignment of cells in various tissues plays a significant role in the maintenance of specific functions. To induce such an alignment, ideal scaffolds should simulate the characteristics and morphologies of natural tissues. Aligned structures that guide cell orientation are used to facilitate tissue regeneration and repair. We here review how various aligned structures are fabricated, including aligned electrospun nanofibers, aligned porous or channeled structures, micropatterns and combinations thereof, and their application in nerve, skeletal muscle, tendon, and tubular dentin regeneration. The future use of aligned structures in tissue engineering is also discussed.

Keywords Aligned structures · Cell orientation · Electrospun nanofibers · Channeled structures · Micropatterns · Tissue engineering

Introduction

Many tissues including muscles [1], vascular tissue [2], and nerves [3] exhibit organized cell alignment. In vivo, the surrounding microenvironment is responsible for cell orientation, dictating the topography, and providing biological signals. This greatly affects cell proliferation [4] and differentiation [5]. Cell alignment plays a significant role in the maintenance of specific functions. For example, the appropriate alignment of cardiac cells is the basis of heart contraction. Tissue engineering researchers have to appreciate the significance of highly oriented cell alignment. Regenerative medicine (the development of tissue and organ substitutes) has made tremendous progress in recent decades [6]. Scaffolds not only provide three-dimensional (3D) structural frameworks but also guide cellular behavior and function [7]. To induce organized cell alignments, scaffolds seek to simulate the characteristics and morphologies of natural tissues [8]. Aligned structures that guide cell orientation have been studied extensively. Such structures control cell behavior by mechanically modulating the cytoskeleton or the physical and chemical gradients involved in extracellular matrix (ECM) formation, facilitating tissue regeneration. One of the representative experiments is that, the neurites of rat dorsal root ganglion neurons cultured on aligned nanofibers are longer and more aligned (along the nanofibers) than cells cultured on randomly oriented nanofibers [9]. Micropatterns mimic cell growth microenvironment during tissue regeneration [10]. A chitosan micropattern with appropriate bridge/groove widths efficiently orientated Schwann cells (SCs) [11]. Other micropatterns directed the differentiation of human-induced pluripotent stem cells [12]. Recently, aligned scaffolds have been used for the regeneration of ligaments/tendon [13], periodontium [14], skin [15], muscles [16], and nerves [17]. Such scaffolds control cell morphology, orientation, and behavior, accelerating tissue regeneration. The scaffolds served as biomimetic (topographically appropriate) ECMs have attracted increasing attention. Here, we review recent progress in the biofabrication of aligned structures that guide cell orientation, the applications of these structures, and future perspectives (Fig. 1). We first describe

Kejie Lu and Ying Qian have contributed equally to this work.

✉ Mengfei Yu
yumengfei@zju.edu.cn

✉ Huiming Wang
whmwhm@zju.edu.cn

[1] The Affiliated Hospital of Stomatology, School of Stomatology, Zhejiang University School of Medicine, and Key Laboratory of Oral Biomedical Research of Zhejiang Province, Hangzhou 310006, China

[2] The State Key Laboratory of Fluid Power and Mechatronic Systems, School of Mechanical Engineering, Zhejiang University, Hangzhou 310028, China

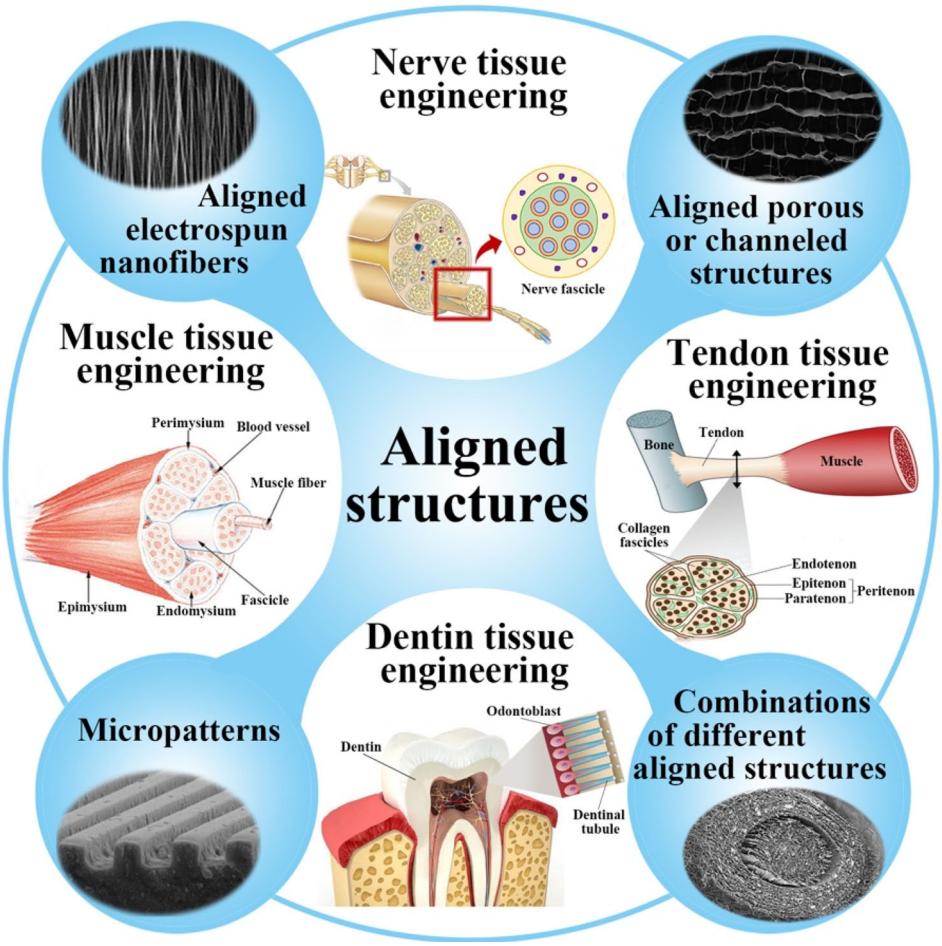

Fig. 1 Schematic of the biofabrication of aligned structures, including aligned electrospun nanofibers, aligned porous or channeled structures, micropatterns and combinations thereof, and their applications in nerve, skeletal muscle, tendon and dentin tissue engineering

the biofabrication of aligned electrospun nanofibers, aligned porous or channeled structures, micropatterns, and combinations of these modalities. We then focus on their applications in nerve, skeletal muscle, tendon, and tubular dentin regeneration. We finally discuss the challenges and future directions.

Fabrication of aligned structures that guide cell orientation

Aligned electrospun nanofibers

Electrospun nanofibers (especially aligned nanofibers) are very promising engineered structures [18–20]; cells align themselves along the fibers [21]. Li et al. compared the cytoskeletons/nuclei of human umbilical vein epithelial cells cultured on different fibrous scaffolds for 1, 3, and 5 days; cell growth followed the fiber direction and cells became elongated along the fiber axis [22]. The fabrication of aligned nanofibers differs from conventional electrospinning. We next briefly introduce both conventional and aligned electrospinning.

Principles of electrospinning

As shown in Fig. 2a, the basic electrospinning apparatus includes a high-voltage–power supply, a power source, and a receptor. High electrostatic forces are used to extract or eject continuous filaments from a polymeric solution through a syringe [23]. Specifically, the polymer fluid is driven into a high-voltage electrostatic field by the syringe. The charge in the electric field gathers at the spinneret to form a conical droplet, called the Taylor cone [24]. When the voltage breaks through the critical point of resistance about surface tension and viscosity of the polymer fluid, the charged jet is ejected from the top of the Taylor cone [25]. It is finally deposited on the receiver device and cured to obtain nanoscale fiber materials, with unstable movement and rapid volatilization of the solvent [26]. This can be simply controlled by varying solution properties (surface tension, viscosity, and concentration), environmental factors (temperature, humidity, and air velocity), and technical parameters (the motion of the grounded target, the applied electrical potential, and the working distance) [27]. All aspects of fiber diameter, porosity, and strength can be controlled [28]. However, the polymer

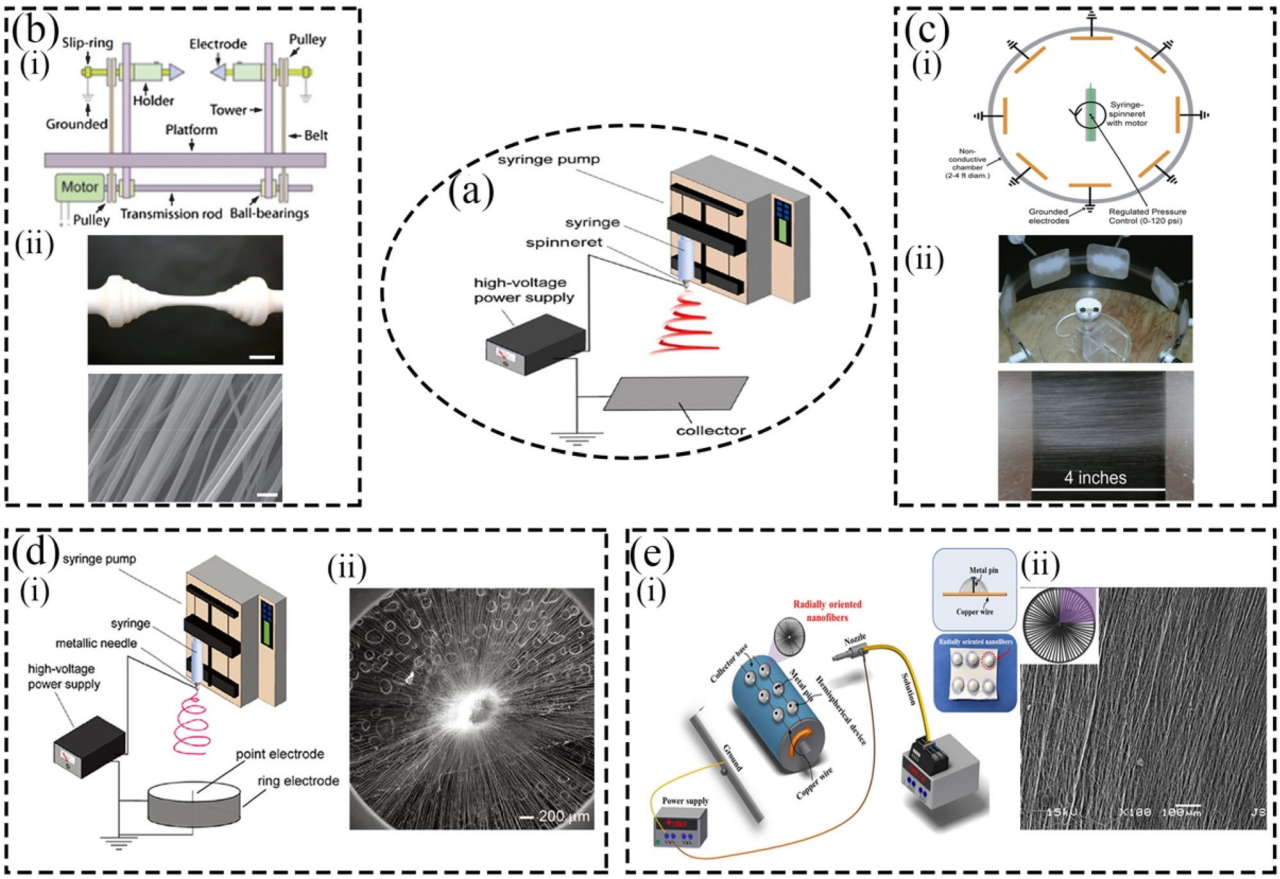

Fig. 2 Fabrication of aligned electrospun nanofibers. **a** Schematic of the electrospinning technique. (Reproduced from [25], Copyright 2017, American Chemical Society) **b** (i) Schematic diagram of a setup used to generate aligned nanofibrous tubes. (ii) Photograph and SEM image of an aligned nanofibrous scaffold deposited between a pair of stepped-cone electrodes. (Reproduced from [42], Copyright 2013, Royal Society of Chemistry) **c** (i) Schematic illustration of the centrifugal electrospinning (CE) system configuration. (ii) Photograph of aligned nanofibers deposited across a four-inch gap between two grounded electrodes. (Reproduced from [45], Copyright 2012, Royal Society of Chemistry) **d** (i, ii) An electrospinning setup employed to generate radially aligned nanofibers, with an SEM image showing the radial alignment. (Reproduced from [47], Copyright 2010, American Chemical Society) **e** (i, ii) Another electrospinning setup used to fabricate such nanofibers, with SEM images of the nanofibers (purple region) [49]

jet extends over the entire rotating collector; the fibers are thus randomly oriented.

Parallel electrospun nanofibers fabricated by modified collectors

Electrospinning can be improved by modifying the collector. For instance, Li et al. used a collector with a gap in the middle [29]. This is formed from two strips of electrically conducting material (e.g., a metal or highly doped silicon) or aluminum foil. The gap width varies from hundreds of micrometers to several centimeters. Electrostatic interaction is exploited to form nanofibers aligned across the gap between (for example) two silicon strips. Based on such work, Shalumon et al. developed a novel, parallel blade collector ensuring a high degree of fiber alignment [30]. The system features two blades with low curvature radii and the sharp edges facing in opposite directions. This increases the magnitude of the horizontal electric field strength, creating a high pull force across the gap. However, fabrication based on an electrical field cannot be scaled up. Hence, Yang et al. developed magnetic electrospinning; two magnets are added to a conventional device [31] and a small amount (less than 0.5 wt%) of magnetic substance is added to the polymer solution. All of the plastic plates used, the gap and polymer solutions with and without a magnetic substance, and magnetic force strength are evaluated. The magnetic field aligns the fibers in parallel; fibers attached to a magnet are stretched. The method is simple, controllable, and efficient. Chen et al. further optimized magnetic electrospinning conditions including the polyaniline (PANi) content and the feed rate [32]. Highly aligned, electrically conductive polycaprolactone (PCL)/PANi nanofibers

are obtained. Nevertheless, the aligned nanofibers generated by the electrostatic/magnetic fields are restricted by a narrow area and limited length, comparing to the application of rotating collectors [33].

The rotating collectors, as a common technique for aligned electrospun nanofibers, include rotating drum collector [34], rotating disc collector [35], rotating wire-drum collector [36], and so on. When it rotates, nanofibers on the collectors can be stretched and thus parallel. The rotating velocity of the collectors could affect the degree of alignment of the nanofibers obviously. If the rotating speed is too high, the nanofibers fracture with high probability [37], while a very low rotating velocity cannot promote the alignment of nanofibers [38]. Therefore, the rotating velocity should be consistent with the fiber spinning rate. Besides, as the rotating velocity increasing, the diameter of nanofibers generally decreases. It is reported that an increase in the rotation speed (from 800 to 2500 rpm) leads to a decrease in the average nanofiber diameter (from 257 to 191 nm) and an increase in the number of fibers with the diameter in a smaller range of 100–250 nm [39]. Moreover, it should be noted that above rotating collector method producing 2D fibrous membranes only and produce less aligned nanofibers with the increase in spinning time [40]. Therefore, based on the rotating collectors, some researchers added the electrostatic field to fabricate highly aligned 3D nanofibrous constructs such as rotating tube with knife-edge collector [41]. As shown in Fig. 2bi, Jana et al. proposed an electrospinning system to fabricate 3D aligned nanofibrous tubes, which has a pair of rotating stepped-cone electrodes [42]. Interestingly, when more fibers are deposited, the outer tubular construct might be slightly concaved (Fig. 2bii). This can be attributed to the change in electrostatic force acting on the fibers. And the degree of concavity is also related to the physical properties of the polymer.

Besides, given the limitation in yield and alignment of aligned nanofibers, the centrifugal electrospinning (CE) system emerges in recent years [43]. As the name implies, the centrifugal electrospinning combines the centrifugal force and electrical force, and thus, it could produce more aligned nanofibers at lower working voltages or slower rotating velocities [44]. For example, Edmondson et al. proposed a hybrid electrospinning system, which is an integration of the parallel-electrode method and centrifugal dispersion [45]. In this technique, a rotating hub hosting a spinneret (or syringe needle) is located at the center and an array of grounded plate electrodes circularly surrounds (Fig. 2ci). Therefore, not only could the rotating spinneret make the solution jet possess additional momentum toward the direction of nanofiber alignment, but also the electrostatic field between the neighboring electrodes could facilitate the alignment of nanofibers. Besides, the width of the gap between the neighboring electrodes determines the length of the aligned nanofibers. Based on the above, this system could produce highly aligned nanofibers over a large area (with fiber length up to several inches) (Fig. 2cii). Recently, a high-throughput centrifugal electrospinning (HTP-CES) system was reported, which makes it possible to produce highly aligned nanofibers at a larger scale [46].

Radially aligned electrospun nanofibers fabricated by novel electrospinning devices

Radially aligned nanofibers are required by tissue engineers studying the cornea, meniscus, and dura mater; Xie et al. are the first to fabricate such fibers [47]. As shown in Fig. 2d, the electrospinning device is conventional in nature, except for the collector, which features a metallic ring electrode and a needlepoint electrode. The electric field vectors (streamlines) in the vicinity of the collector differ from conventional streamlines, being split into two fractions attracted to the ring and point electrodes. Stocco et al. developed a novel electrospinning device [48] by modifying the collector to include an external hollow cylinder with a central pin and a mobile, internal hollow cylinder. The electric field vectors are as described above; thus, a peripheral ring and a center point. Radially aligned nanofibers are generated on the spinning, internal hollow cylinder. Recently, as shown in Fig. 2e, Kim et al. developed a novel method using a single nonconductive hemispherical device and a metal pin to fabricate 3D hemispheres of radially aligned nanofibers [49]. The collector is "peg-top-shaped"; thus, a hemispherical nonconductive device with a metal pin in the center and a circle of copper wire around the edge. Several such devices are placed on a modified rotating collector to manufacture hemispherical 3D forms with radially aligned nanofibers, thus adding an extra dimension to 2D electrospinning.

In addition to the parallel and radial electrospun nanofibers, considering the diversity of the morphology and arrangement structure of cells of natural tissues and organs, electrospun nanofibers with different arrangements should be designed according to the aimed tissues. It would have a greater application demand in the practical biomedical field. Therefore, the combination of electrospun nanofibers and micropatterns emerges, which would be introduced below.

Aligned porous or channeled structures

Such structures are fabricated via directional freezing (also termed "ice templating" or "freeze-casting"). For example, chitosan–alginate (C/A) polyelectrolyte complex scaffolds fabricated via directional freezing exhibit aligned, linearly porous structures [50]. Chick dorsal root ganglia growing on C/A scaffolds extends most neurites parallel to the longitudinally oriented channels. Similarly, 3D silk fibroin scaffolds with longitudinal multi-channels guide the growth of hip-

pocampal neurons parallel to the channels [51]. Thus, aligned porous or channeled structures on scaffolds physically guide cell orientation.

Principles of directional freezing

Directional freezing uses temperature gradients to control the movement of frozen primitives (Fig. 3ai). First, the reaction precursors are dissolved or dispersed in water. Next, the mold containing the solution is placed on a low-temperature (below freezing point) platform. The solvent nucleates and crystallizes along the direction of the vertical temperature gradient, thus from the cold stage to the top, forming oriented ice crystals. The solute is repelled by the ice crystals and thus becomes squeezed among them. Aligned porous or channel structures are obtained after removing the ice crystals via freeze-drying (Fig. 3aii). The solid content [52], polymer molecular weight [53], and freezing temperature [54] affect the direction, quantity, morphology, and size of the porous or channeled structures. Such directional freezing has been applied to fabricate hydrogels [55], aerogels [56], ceramics [57], and composite materials [58].

Scaffolds with highly directionally aligned microstructures fabricated by magnetic freeze-casting

Inspired by the helicoidal structure of the narwhal tusk, Porter et al. introduced the novel concept of magnetic freeze-casting [59]. They apply a magnetic field to a conventional freeze-casting system for the first time, which allows the interconnected pore channels to be aligned in two directions: (1) the ice growth direction and (2) the magnetic field direction. The key to the magnetic freeze-casting is the interaction of magnetic material in casting solutions with an external magnetic field. On this basis, different magnetization orientations are designed by putting different magnets together, including radial magnetization, axial magnetization, and transverse magnetization (Fig. 3bi) [60]. The different magnetic fields would yield different alignment microstructures in freeze-cast materials, such as "core–shell" structures, "core–shell" gradient architecture, lamellar walls and mineral bridges (Fig. 3bii). As shown in Fig. 3biii, the transverse magnetic field could make substantial mineral bridge alignment, whose orientation is parallel to the field direction. These alignment microstructures could enhance the mechanical properties of freeze-cast scaffolds, which may meet the requirement of bone regeneration scaffolds. Recently, some researchers proposed a single Helmholtz coil [61], even a triaxial nested Helmholtz coils [62] instead of permanent magnets to generate a more uniform magnetic field. The uniform magnetic field could avoid particle agglomeration and thus lower the risk of unintended stress concentration in the scaffolds. Meanwhile, the uniform magnetic field could also increase mechanical characteristics, because of the more generation of lamellar walls in the compression direction. The unique advantage of the triaxial nested Helmholtz-coils-based freeze-caster is the ability to control the magnetic field in any direction at any time. In a word, the magnetic freeze-casting may enable the development of biomimetic bone scaffolds that mimic both the structure and mechanical properties of natural bone.

Aligned lamellar porous scaffolds fabricated by electric field freeze-casting

It has been reported that particle would move during freeze-casting electric fields [63]. Hence, researchers are interested in whether it was possible to control the direction and consistency of the pore or channels via adjusting the direction and intensity of electric fields. Tang et al. found that the direction and size of ice crystals were depended on the temperature gradient and different electrostatic field intensities. Further study revealed that the direction of the pore or channels was a vector sum of the temperature gradient and electrostatic field intensity [64]. Based on the above, a novel fabrication combining directional solidification with electrostatic fields is proposed to manufacture aligned lamellar porous scaffolds. Recently, according to the action of the temperature gradient, electric fields and magnetic fields in freeze-casting, a novel fabrication integrating directional solidification, multiple cold sources, electrostatic field, and the magnetic field is used to fabricate porous scaffolds with aligned distribution pore or channels and high mechanical properties, which could help to obtain aligned porous or channeled structures with higher strength [65].

Large-scale aligned porous structures fabricated by bidirectional freezing

Directional freezing has improved over the years. To generate large, porous, aligned lamellar structures, Bai et al. developed a novel bidirectional freezing technique [66]. The key tools are PDMS wedges with different slopes. Whereas directional freezing features only one (vertical) temperature gradient, bidirectional freezing features both vertical and horizontal gradients because the wedges isolate the slurry from the copper substrate. Ice-crystal formation is manipulated in two directions by adjusting the slope angle and cooling rate.

Radial hydroxyapatite scaffolds fabricated by radial freeze-casting

Radial freeze-casting is used to fabricate radial hydroxyapatite scaffolds [67]. The ice crystals grow from the center to the edge of the mold. The lamellar spacing becomes wider nearer the mold. Similarly, a cylindrical mold with sides and

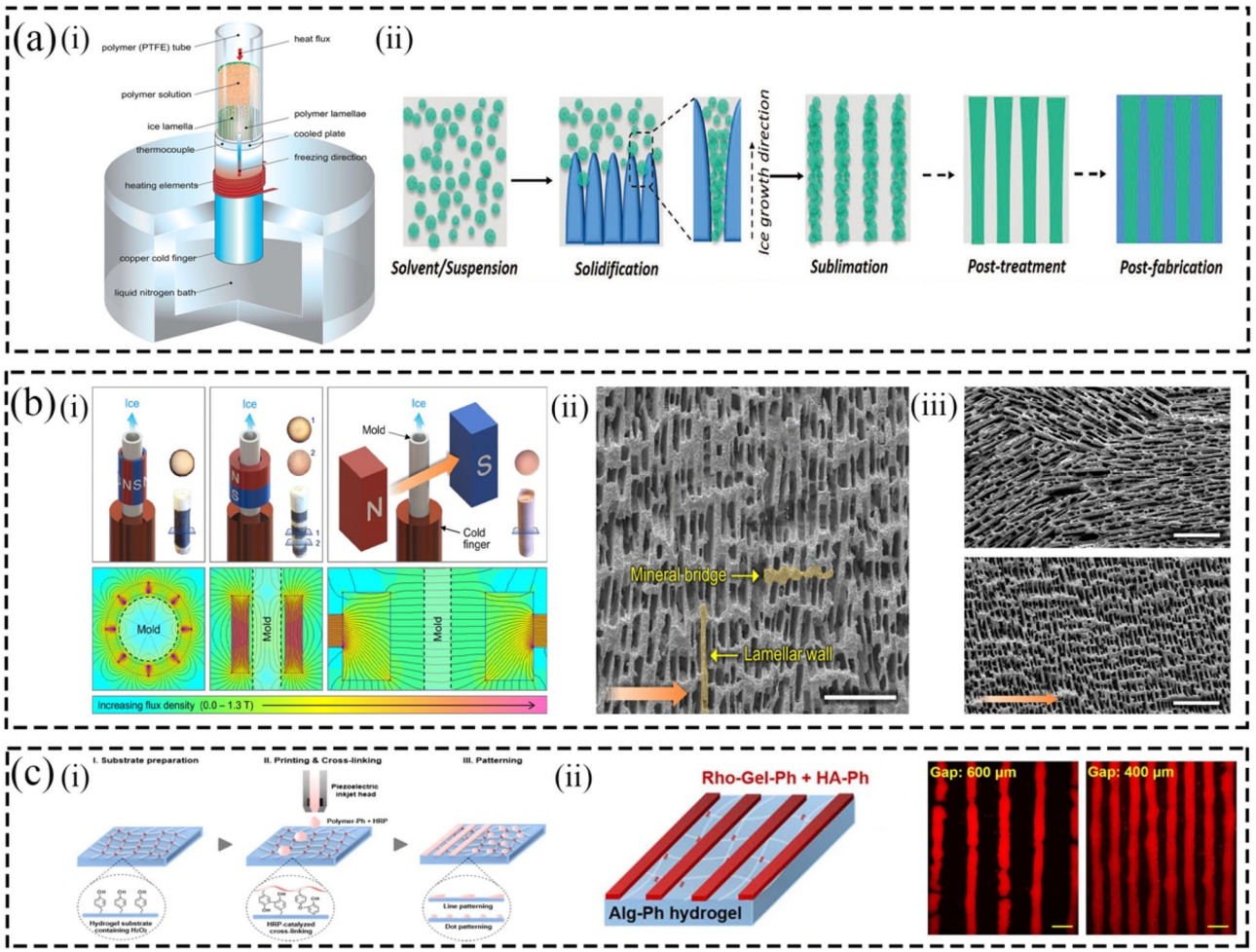

Fig. 3 Methods used to fabricate aligned porous or channeled structures and micropatterns. **a** (i, ii) Schematic of directional freezing and performance. (Reproduced from [50, 70], Copyright 2013, John Wiley and Sons and Copyright 2020, John Wiley and Sons) **b** (i) Schematics and finite element models of the three different magnetization orientations with respect to the freezing mold and copper cold finger. (ii) An image of different alignment microstructures in freeze-cast materials, including lamellar walls and mineral bridges. (iii) Representative micrographs of scaffolds freeze cast under (up) no magnetic field and (down) a transverse magnetic field of 0.09 T. The ice growth direction is out of the page, and the orange arrow indicates the direction of the magnetic field. (Reproduced from [60], Copyright 2016, John Wiley and Sons) **c** (i) Schematic of micropatterning using inkjet printing and horseradish peroxidase-catalyzed hydrogenation. (ii) Fluorescence microscopy images of lines containing Rho-Gel-Ph and HA-Ph of different gap widths formed on an Alg-Ph hydrogel; the image was taken just after printing. (Reproduced from [97], Copyright 2020, IOP Publishing) Rho, rhodamine. Gel, gelatin. Rho, rhodamine. Ph, phenolic hydroxyl. HA, hyaluronic acid. Alg, alginate

bottom made of conductive metal is designed. The mold can promote the distribution of ice crystals along the radial direction and thus fabricate aligned lamellar porous alumina with a radial structure [68]. 3D scaffolds with aligned macrochannels composed of radially aligned nanofibers are created via guided ice-crystal growth [69]. The technique has tremendous potential in terms of structural control.

In conclusion, the directional freezing is particularly effective toward the fabrication of biomimetic structures, which are often characterized by aligned porous or channeled structures. However, all porous materials have an inherent lack of strength associated with porosity [70], which should be concerned with.

Micropatterns

Micropatterning is first applied in microelectronics, and then in biology, as a powerful tool for the study of cell behavior. For instance, given the similarity between micropatterned substrates and tissue architecture, many scholars study cell migrate on the subject [71–74]. Cell migration patterns are classified as aligned, confined and the combination of the two, when cultured on micropatterns. And some studies

demonstrated that cell migration direction is manipulated by the divergence angle of micropatterns and cell migration speed is controlled by the width of micropatterns [75]. Besides, micropatterns induce mechanotransduction and cause distortions and deformation in the cell morphology, even in the nuclei [76, 77]. Another study showed that cell morphology could influence cell fate indirectly [78]. Generally, biological micropatterning includes chemical structural patterning and topology-based physical patterning [79]. Some micropattern regions may repel cells; other regions attract cells (that then adhere) [80, 81]. Hence, cells form certain patterns and can thus be orientated.

Micropatterns by lithography-based techniques

Photolithography is a highly sophisticated fabrication with a resolution of 1–2 μm for micropatterns. The region (patterns) on a photomask (a film that enables passage of the UV light through unmasked regions) can be duplicated onto a substrate (a silicon wafer generally) via UV exposure [82]. The depth of the micropattern in the stamp is dependent on the thickness of uncross-linked photoresist spin coated on the substrate and thus can be adjusted [83]. Recently, Chen et al. designed different hybrid micropatterns through UV lithography and nanoimprinting approaches and focused on the interaction between photoreactive polymer polyvinyl alcohol (PVA)-micropatterned surface and mesenchymal stem cells (MSCs) [84]. They found the width of micropatterns can influence cell orientation, morphology, even osteogenic and smooth muscle differentiation of MSCs. Interestingly, adipogenic differentiation has no evident relationship with the spacing and orientation of micropatterns. However, the photolithography approach requires expensive facility and a clean room environment for manufacturing micropatterns, which make it difficult to spread in the field of biology. Therefore, soft lithography emerges, which create micropatterns by an elastomeric ("soft") material such as poly (dimethylsiloxane) (PDMS) [85]. This technique has a lower request for a clean room and the same original wafer can produce multiple stamps by replica molding procedure. Compared to photolithography, it is lower cost and easer. Deserved to be mentioned, microcontact printing, as a soft lithographic approach, can generate molecular-level chemical micropatterns on a surface [86]. However, it cannot be achieved in conventional photolithography easily. Because it requires complex surface modifications generally [87]. Recently, Friguglietti found that the combination of Si and TiB_2 micropatterned substrates can influence the alignment of cells directly [88]. The key role is the differential adsorption of proteins on Si and TiB_2 substrates. The biofabrication process is simple and amenable to scale up, because of the simple surface modification processes.

Micro- and/or nanoscale ridge/groove pattern arrays fabricated by CFL

Macadangdang et al. developed two controllable, cost-effective, and scalable nanopatterning processes for cardiac tissue engineering [89]. Both feature CFL (UV-assisted or solvent-mediated). Poly(lactide-co-glycolide) (PLGA) or polyurethane (PU) is placed on a glass coverslip, and a polyurethane acrylate (PUA) mold is then placed on top. UV radiation (λ = 250–400 nm), or heat (120 °C) and pressure (100 kPa), are used for curing, and the mold is then peeled off. Neonatal rat ventricular myocytes growing on nanopatterns are aligned; control cells are not. Similarly, Lee et al. fabricated PUA nanoscale ridge/groove arrays via UV-assisted CFL [90]. Scanning electron microscopy (SEM) reveals almost no variation in dimensions or alignment angle; the method yields high-quality nanoscale ridge/groove pattern arrays. However, these micropatterns are only constructed at a single (micro or nano) scale, limiting the nanogroove aspect ratios and depths, in turn compromising cell alignment. Two-step, UV-assisted capillary molding techniques were thus used to fabricate micro-/nanoscale hierarchical polymers [91]; two-scale molds are employed sequentially during UV-assisted molding. In such approaches, a UV exposure time ensuring only partial curing after the first step is essential. Similar methods were described by Li et al. [92] Two-stage UV imprinting is used to fabricate a two-layer polydimethylsiloxane (PDMS) mold that replicated hybrid patterns. The critical parameters are the operating load and irradiation time. When nano- and microscale patterns are both present, cells are orientated along the nanogrooves.

Tailor-made and sophisticated 3D micropatterns fabricated by the laser-based technique

Wavelength- and power-tunable lasers have many applications in micropatterning. Lu et al. laser-scribed 3D graphene-based micropatterns [93]. A LightScribe DVD burner and a standard DVD are used to manufacture custom 3D wafer-scale (~ 100 cm^2 area) graphene patterns. Fabrication is simple and rapid. First, the disk is covered with a layer of graphene oxide (GO) film on an arbitrary substrate and placed in the DVD burner. Then, the print mode, gray value, contrast, and repeat time are set. The customized 3D graphene-based micropatterns range from the microscale (even nanoscale) to decimeters. A two-dimensional fast Fourier transform shows that the micropatterns directed cell alignment. Ma et al. developed an innovative, laser-guided, maskless micropatterning technique [94] using laser-capture microdissection to fabricate a tubular architecture for the first time, which will aid the tubular regeneration of dentin and nephrons.

Hydrogel micropatterns fabricated by the piezoelectric inkjet printing technique

Many micropatterning methods exist; all are imperfect [95]. For example, photolithography [96] requires UV treatment, elaborate equipment, and multiple steps. Inkjet printing allows organized cell alignment using micropatterns created via non-contact liquid deposition. Recently, Gantumur et al. developed an inkjet micropatterning featuring horseradish peroxidase (HRP)-mediated (rapid) hydrogenation (Fig. 3ci) [97]. When ink contacts the substrate, the ink polymers possessing phenolic hydroxyl moieties (Polymer-Ph) and non-cross-linked phenolic hydroxyl (Ph) in the substrate form cross-links via the HRP-mediated reaction. Gaps of different widths are created to determine how to optimally align cells with the patterns (Fig. 3cii).

Although the micropatterning approaches have made great progress, the drawback of them still exist. For instance, micropattern structures cannot contain protein or growth factors. The active proteins would denature because of the micropatterning methods involve UV light and laser. Furthermore, micropatterns only have surface morphology, so it has difficulty to form a 3D structure, which would restrict their application in tissue engineering.

Combinations of aligned structures

Soft lithography [98], microcontact printing [99], and reactive ion etching [100] have been used to create electrospun fiber patterns. We focus here on the combination of electrospun fibers and micropatterning and the combination of electrospun fibers and freeze-drying. In general, electrospun nanofibers are circular in cross section and have a smooth surface. A rough surface (a topographical cue) would promote cell adhesion [101]. Hence, secondary oriented structures on nanofiber surfaces have received attention. Huang et al. fabricated nanofibers with a parallel-line surface texture via electrospinning of cellulose acetate butyrate (CAB) [102]. The CAB concentration, the volume ratio of acetone to DMAc, electrospinning distance, and molecular weight of CAB affect fiber surface morphology. Parallel-line surface morphology is obtained via rapid evaporation of a highly volatile solvent (acetone) and a long electrospinning time. The parallel-line surface structure promotes SC alignment and extension. The highly ordered secondary structure formed by the surface grooves plays a significant role. The surfaces of nanofibers fabricated via photolithography [103, 104] and micromolding [105] have also been modified. For example, Zhang et al. fabricated aligned PCL scaffolds by combining micropatterning with electrospinning [105]. First, PDMS stamps with ridge/groove structures are fabricated via micropatterning of silicon panels, and the stamps are coated with a thin layer of gold. PCL is then spun onto the stamps using an in-house electrospinning platform. Optical microscopy and SEM reveal that the PCL solution flow rate greatly affects PCL micropatterning. As the flow rate increases, the ridge/groove micropatterning becomes clearer, but the fibers become randomly orientated. In vitro, SCs grew in the micropattern direction. Guex et al. fabricated micropatterned matrices of parallel-oriented fibers using a rotating drum with an engraved relief [106]. The electrospun scaffolds exhibit a wavy structure of grooves and ridges, reflecting the surface of the relief. The nanofibers are parallel and the wave topographic boundaries not obvious. Myoblasts grow along the grooves. Currently, there are relatively few researches on the micropattern structure of electrospun fibers, and most of these researches focus on the observation that the micropattern structure of electrospun fiber would have a positive impact on the growth behavior of cells. The mechanism of regulation of cell behavior is less elaborated.

As aligned nanofibrous scaffolds feature dense fibers, both cell infiltration and cell–scaffold interaction are compromised. Mechanically, such scaffolds are weak; specifically, they resist axial compression poorly. Ma et al. fabricated a nanoyarn-porous nanofiber hybrid scaffold (HS) by combining electrospinning and freeze-drying [107]. First, conjugated electrospinning is used to produce an aligned nanoyarn scaffold employing two oppositely charged nozzles. Next, uniform dispersion of nanofibers is poured over the scaffold and a mold applies. A 3D, porous, nanofibrous/nanoyarn HS is obtained after freeze-drying and cross-linking. The HS exhibits larger pore size and greater porosity than the aligned nanofibrous scaffold, facilitating cell infiltration; the number of bone marrow stromal cells (BMSCs) cultured on the HS is significantly higher than that on the aligned nanofibrous scaffold. The HS exhibits high tensile and compressive strengths. However, although some BMSCs attach to the inner HS region, the cells are not uniformly distributed; this is a challenge for the future.

Tissue engineering applications

Compared with random structures, aligned structures could provide special topography and thus guide cell orientation. It has been reported that aligned structures can control morphology, behavior and functions of cells [108, 109]. Hence, considering potentials of aligned structures in regulating cell behaviors, a growing number of aligned structures are applied in tissue engineering. In this section, these possible applications will be briefly introduced, including nerve, skeletal muscle, tendon and tubular dentin regeneration.

Nerve tissue engineering

The brief introduction to nerve

Generally, each nerve fiber is covered by a dense layer of connective tissue called epineurium. More importantly, the multiple nerve fibers covered by endoneurium are orientated in axial alignment to form a nerve fascicle. Similarly, the perineurium, which mainly protects and separates the nerve fibers, wraps nerve fascicles. Due to the division of the perineurium, the nerve fibers with the same function and orientation are gathered together to form cords, which play the function of nerve conduction orderly. Hence, the directionality of nerve fibers is crucial to the function of the nerve [110]. Currently, more and more traumatic peripheral nerve injuries (PNI) often result in deterioration and loss of motor, sensory, and autonomic functions [111, 112]. However, due to the limit of regeneration capacity and the complication of the healing process, the treatment of PNI is difficult [113].

The applications of aligned structures

Given the directionality of nerve fibers, the aligned structures, as contact topographical cues, would promote the cellular migration and alignment and thus enhance axonal regeneration [114]. Therefore, inspired by the structure of nerve, aligned nanofibers and oriented micro-channels have been applied in bionic nerve guide conduits (NGCs). Based on the similarity between aligned nanofibers and nerve fibers, aligned nanofibers have been used to create the inner walls of NGCs. To impart structural support, randomly oriented nanofibers are employed to make the outer NGC layers. As shown in Fig. 4ai, Kim et al. presented a one-step fabrication method using both aligned and randomly oriented nanofibers [115]. An NGC can be divided into three parts—the proximal and distal portions (with aligned nanofibers), the exterior medial portion (with random nanofibers), and an aligned nanofiber interior (Fig. 4aii–iii). In vitro, nerve cells tend to grow along the aligned nanofibers (Fig. 4aiv). In vivo experiments have not been reported. Zhu et al. fabricated a bilayer NGC [116]. Sciatic nerve defects (1 cm) are created in rats that are divided into three different groups that receive randomly oriented nanofibrous NGCs, aligned nanofibrous NGCs, and autografts. Nerve regeneration at 2 and 12 months post-surgery is analyzed histomorphometrically and electrophysiologically. The bilayer NGC is superior to the random NGC and exhibits similar performance as an autograft. Besides, given that longitudinally oriented microstructures fabricated via unidirectional freezing are similar to nerve-guiding, basal laminar microchannels, longitudinally oriented NGCs have been developed to facilitate continuous linear axonal growth along oriented micro-channels [117]. Zhang et al. combined collagen-chitosan NGCs with longitudinally oriented micro-channels (L-CCH) and SCs [118]. NGCs with L-CCH, with or without SCs, are implanted into 15-mm-long sciatic nerve defects in rats, and SC morphologies are evaluated at 3 days and 1 and 2 weeks later via SEM. SCs adhere to and migrate into the L-CCH to become longitudinally aligned along the microchannels, forming the bands of Büngner associated with peripheral nerve regeneration. The SFI, and electrophysiological and histological evaluations, show that L-CCH promotes axonal regeneration and functional recovery.

Furthermore, based on the effects of micropatterns mentioned above, micropatterns such as grooves have been applied to NGCs to promote nerve regeneration. Huang et al. developed a fibrous NGC featuring electrospun nanofibers with multiple longitudinal grooves [119] fabricated from CAB, which exhibits good biocompatibility. In a model of sciatic nerve injury, the electrophysiological results, gastrocnemius muscle evaluation, walking track test, and immunofluorescence showed that grooved CAB is better than smooth CAB, attributable to the fact that the grooves delivered topographical cues promoting linear cell growth. Besides, as shown in Fig. 4bi, Zhang et al. reported a novel NGC with micropatterns (physical cues) on an inner wall formed from GO nanosheets that deliver biochemical cues [120]. Micropatterned, GO-modified poly(D, L-lactide-co-caprolactone) (PLCL) films significantly enhance the directional migration of single cells (Fig. 4bii–iv). Sciatic nerve defects (10 mm) in rats bridged using different NGCs and autografts are evaluated both histologically and functionally. The sciatic function index (SFI), compound motor action potential, nerve conduction velocity, immunofluorescence staining profile, and microstructural quality afforded by 3/3-GO conduits (GO nanosheets with ridges/grooves 3/3 μm in dimensions) are similar to those of autografting, and better than those of the 3/3 and flat/GO groups (Fig. 4bv).

However, most of NGCs mentioned above are hollow. The main drawback of them is the incapacity of controlling the dispersion of the axons, which cannot bridge larger nerve gaps. Hence, cell-aligned structures (fillers) have been added to NGCs; these include electrospun, aligned fibrous matrices [121], and materials prepared via unidirectional freezing [122, 123]. Electrospun fibers may be subjected to freeze-drying. As shown in Fig. 4ci–ii, Huang et al. developed NGCs with oriented collagen/chitosan (O-CCH) fillers fabricated via directional freezing [124]. The NGC sheaths are composed of electrospun PCL. SCs and axons cultured on O-CCH fillers exhibit directional growth and migration (parallel to the oriented micro-channel wall), whereas cells cultured on random collagen/chitosan (R-CCH) fillers do not (Fig. 4ciii). In vivo, O-CCH accelerates axonal regeneration and SC migration, delivering longitudinal guidance cues (Fig. 4civ). Shah et al. also designed a multi-channel

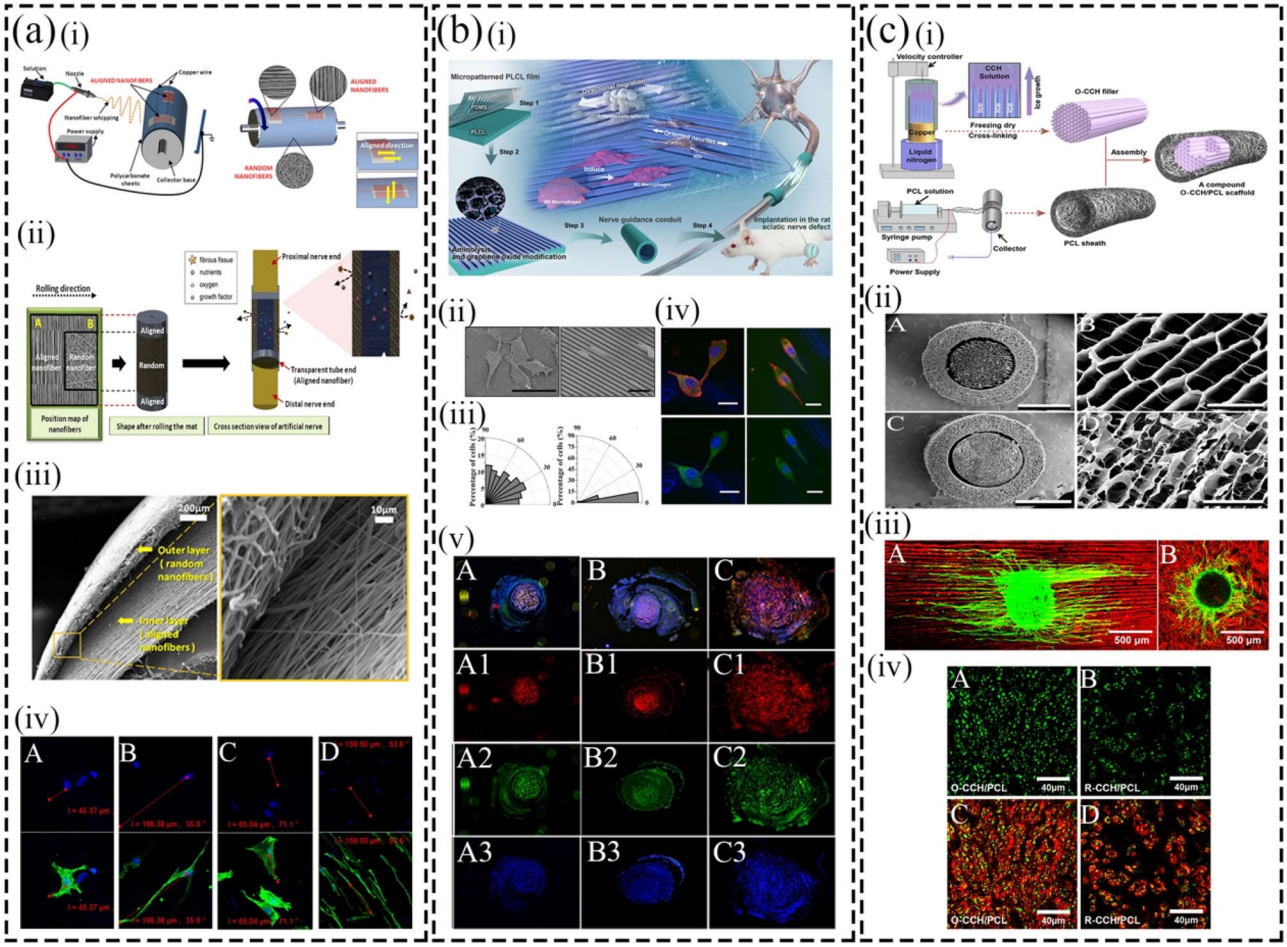

Fig. 4 **a** (i) Schematic illustration of fabrication for the controlled design of aligned and randomly oriented nanofibers. (ii) Schematic 3D illustration of the nerve guide conduit. (iii) SEM images of the cross-section view of the nerve tube. (iv) Confocal microscopy images of PC12 cells attached after (A, B) 1 day and (C, D) 5 days of culture on a randomly oriented and aligned nanofibrous PLGA scaffold [115]. **b** (i) Schematic illustration showing the fabrication of PLCL film with stripe micropatterns and GO nanosheets and its application for guiding the nerve regeneration in vitro and in vivo. (ii) SEM images after Schwann cells were seeded for 12 h flat/GO and 3/3-GO films. (iii) Distribution of SCs orientation angle to the stripe direction after being cultured for 12 h GO modified PLCL films: flat and 3/3. (iv) Merged immunochemical staining images (green, vinculin; red, F-actin; blue, nuclei) of SCs after being cultured for 12 h on GO modified PLCL films: flat and 3/3. (v) Assay of the microstructures of regenerated nerves in vivo. Merged immunofluorescence staining images of (A1–C1) S100β (for SCs), (A2–C2) NF200 (for axons), and (A3–C3) DAPI (for cell nuclei) in the middle segments of regenerated nerves by (A) flat/GO, and (B) 3/3-GO conduits and (C) autografts post-surgery in vivo for 8 weeks. (Reproduced from [120], Copyright 2020, American Chemical Society) **c** (i) Schematic illustration of the stage-wise fabrication of CCH/PCL scaffolds with uniform longitudinally oriented micro-channels. (ii) SEM characterization of the CCH/PCL scaffold. (A) Transverse section of the O-CCH/PCL scaffold displaying tightly matched O-CCH filler and PCL sheath. (B) Transverse section of O-CCH filler. (C) Transverse section of the R-CCH/PCL scaffold. (D) Transverse section of the R-CCH filler. (iii) Axonal regeneration and SC migration on the CCH microstructured filler. DRG explants were seeded on the longitudinal sections of the O-CCH (A) or R-CCH scaffold (B). Axons were labeled with b-tubulin (green); the O-CCH filler exhibited autofluorescence (red). (iv) Long-term nerve regeneration beyond the grafts in vivo. Regenerated nerves at the distal stumps in the O-CCH/PCL (A, C) and R-CCH/PCL (B, D). SCs were labeled with S100 (red), and regenerated axons were labeled with NF200 (green). (Reproduced from [124], Copyright 2017, Elsevier)

spiral NGC [125] featuring internal, longitudinally aligned nanofibers; this is novel.

Perspectives and outlook about nerve regeneration

Taken together, aligned structures, including aligned nanofibers, longitudinally oriented microchannels and micropatterns, have been applied to fabricate directional NGCs. The directional NGCs are designed to simulate the microenvironment of natural nerve tissue and meet the characteristic size of nerve cells. According to applications of aligned structures mentioned above, directional NGCs improve the space utilization of catheter lumen, increase the contact area of NGCs wall, and thus increase the adhe-

sion of SCs to NGCs. Meanwhile, the applications of aligned structures guarantee a higher mechanical property of NGCs, avoiding deformation and subsidence when NGCs are used in vivo. More importantly, they guide distal axon directional growth, reduce the dispersion of the nerve regeneration process, and thus improve the efficiency of nerve regeneration and signal transduction. However, the limitation of different aligned structures still exists. For example, the fabrication of bilayer NGCs is time-consuming with low productivity. And the fabrication process cannot be effectively controlled due to too many unstable factors, which is a challenge for the stable and efficient preparation of bilayer NGCs. Besides, NGCs with micropatterns on an inner wall may lead to an inflammatory reaction, nutrition leakage, or neurite exogenesis more easily than non-micropatterned NGCs. Because the most fabrication of NGCs with ridge/groove distribution on an inner wall has the following two steps, including rolling the films to a cylinder and gluing or sealing the edge of the cylinder. It would generate the suture thread and suture impression of the conduit sidewall. Therefore, it is difficult to fabricate an integral conduit with micropatterned inner wall and seamless sidewall using. In addition, how to effectively fabricate different microgroove morphologies should be further discussed, as well as the influence of micropattern fabrication on the molding quality of NGCs. Considering nerve fibers can be divided into the motor and sensory fibers, the regenerated fibers should re-innervate the desired motor or sensory targets, respectively. But for now, NGCs are incapable of selectively guiding motor and sensory axons, which provides a new direction for the future development of NGCs.

Skeletal muscle tissue engineering

The brief introduction to skeletal muscle

Compared to another two kinds of muscles, skeletal muscle is the most widely distributed muscle, accounting for about 40% to 45% of body weight. Skeletal muscle is composed of a large number of muscle cells with the ability to contract. Muscle cells are fibrous and have multi-nuclear structures. They can produce axial contraction while receiving nerve signals. The most prominent characteristic of them is that they have a high degree of orientation, which is the foundation of contraction. In response to minor injuries, skeletal muscle has the regeneration capacity. However, the capacity of regeneration could not meet the demands for severe damage and disease which would cause loss of muscle and function [126]. Thus, tissue engineering is developing fast, as a promising approach for severe muscle injury and myopathy [127]. To acquire the proper alignment of myofibers, the researches about scaffolds topographical cues have been reported over the years [40].

The applications of aligned structure

Aligned nanofibers have been used to create myotubes that in turn align myoblasts. Notably, smaller-diameter fibers promote myoblast differentiation but not proliferation [128]; fiber diameter directly affects cell stiffness and the contact area. Electrospun, fibrin microfiber bundles hosting C2C12 myoblasts [129] or adipose-derived stem cells/SCs [130] promoted regeneration of murine volumetric muscle loss after partial removal of the tibialis muscle. C2C12 myoblast cells become embedded into aligned alginate fibers, remain viable, and elongate and align along the fibers, facilitating myogenic differentiation [131]. Based on the cell electrospinning technique mentioned above, Guo et al. developed a cell-laden wet-electrospinning method [132]. Thrombin and fibrinogen combine to form fibrin microfibrils that are stretched and aligned via bath rotation. Immunostaining of a cell-laden scaffold shows that the C2C12 cells are viable and highly aligned. The myotube density is low; this will be addressed in the future. However, single fibers cannot form 3D structures that mimic skeletal muscle. A photocurable hydrogel shell [133], PCL melt-plotted struts [134], and 3D-printed PCL struts [135] have been combined with electrospun fibers to mimic native muscle. As shown in Fig. 5ai–ii, Lee et al. developed a novel composite scaffold consisting of outer electrospun decellularized extracellular matrices modified by methacrylate (dECM-MA) nanofibers and inner 3D-printed PLGA struts [136]. The results of staining with DAPI/phalloidin and SEM showed that the human muscle progenitor cells (hMPCs) and F-actin have clearer alignment along the fiber direction (Fig. 5aiii). And the increase in cell differentiation indicators such as the staining results of the myosin heavy chain (MHC), fusion index and the expression of muscle-specific genes demonstrated to the positive effect of the composite scaffold on myogenic differentiation (Fig. 5aiv). Overall, the microscale patterns of PLGA struts and the nanoscale of dECM-MA fibers could facilitate the alignment and compactness of cells, even promote the formation of organized myotube [137].

Similarly, microgrooves (aligned topographical cues) not only promote parallel alignment of C2C12 myoblasts but also facilitate the expression of myogenic differentiation genes (MHC and myogenin) [16]. For C2C12 myoblasts, a 50-μm line pattern optimally promotes alignment and differentiation [138]. Microgrooves are combined with photocrosslinkable GelMA fibers via microfluidic spinning [139]. The effects of nanoscale, wavy surface textures on C2C12 mouse myoblast cells are similar to those of microgrooves [140]. Notably, when wavy surface textures of various topographic sizes ($\lambda = 1520$ nm and $A = 176$ nm to $\lambda = 9934$ nm and $A = 2168$ nm) are analyzed, human myoblast alignment and differentiation do not depend on wavelength or amplitude, unlike what is found when mouse myoblasts are studied [141, 142].

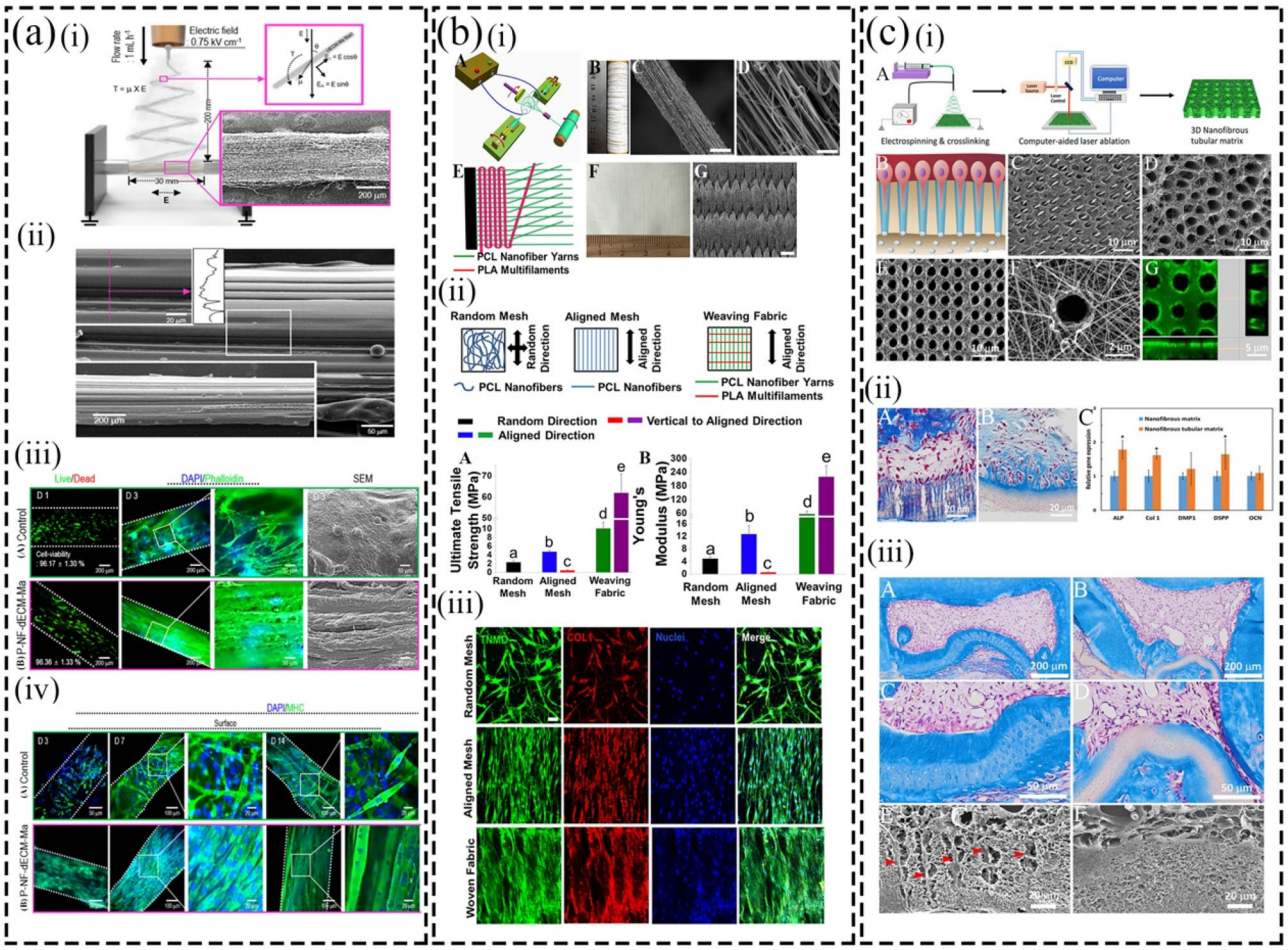

Fig. 5 **a** (i) Schematic of electrospinning on fibrillated PLGA struts and fibers aligned using an electrostatic torque (with an SEM image of the surface topography of PLGA). (ii) Fibrillated PLGA surface supplemented with PVA and fabricated by 3D printing. (iii) Live (green)/dead (red) images at 1 day and DAPI (blue)/phalloidin (green) and SEM images at 3 days for (A) control and (B) P-NF-dECM-MA structures. (iv) DAPI/MHC fluorescence images at 7 and 14 days of (A) control and (B) P-NF-dECM-MA scaffolds. (Reproduced from [136], Copyright 2019, American Chemical Society) **b** (i) Fabrication of PCL nanofibrous woven fabrics. (A) Schematic illustration of the modified electrospinning system for fabricating PCL nanofiber yarns. (B) Photograph of a PCL nanofiber yarn package produced about 2 h. (C, D) SEM images of the electrospun PCL nanofiber yarns. (E) Schematic of the textile weaving process. (F) Photograph and (G) SEM image of the PCL nanofibrous woven fabrics. (ii) Uniaxial tensile testing of PCL nanofibrous woven fabrics and electrospun random and aligned meshes, including (A) Young's modulus and (B) tensile strength. (iii) Woven fabrics promoted HADMSC differentiation toward tenocytes in TDM after 14-day culture. (Reproduced from [155], Copyright 2017, Elsevier) **c** (i) Design, fabrication, and characterization of micropatterned tubular 3D matrix. (A) Schematic of the electrospinning and laser-guided micropatterning processes to fabricate 3D nanofibrous tubular gelatin matrices. (B) Schematic of odontoblasts aligned on the interface between dentin and pulp and the extension of their long processes deep inside the dentinal tubules. (C, D) SEM images of human tubular dentin. (E) A typical SEM image of the micropatterned tubular gelatin matrix. (F) High magnification of showing the nanofibrous gelatin matrix. (G) Confocal image of the tubular gelatin matrix. (ii) (A, B) Trichrome staining after the cell/matrix constructs were cultured in vitro in different media for 2 weeks. (C) Comparison of gene expression of DPSCs on the micropatterned and non-patterned gelatin matrix. (iii) Regeneration of tubular tissues in vivo using a 3D micropatterned matrix. Masson's trichrome staining and SEM images for (A, C, E) tubular matrix group and (B, D, F) non-patterned control group. (Reproduced from [94], Copyright 2018, John Wiley and Sons)

Perspectives and outlook about skeletal muscle regeneration

In conclusion, aligned nanofibers and micropatterns can present aligned topographic cues to myoblasts, which can guide myoblast behavior. Whether the dimensions of microscale topographic features are appropriate for the size of myoblasts is the key for myoblasts orientation. Meanwhile, aligned nanofibers and micropattern can also support fusion and differentiation of myoblasts into highly aligned, densely packed myotubes. However, there are still some deficiencies in the current study. For instance, the aligned cell sheets can

be fabricated via micropatterns is relatively thin, which has large gap with the natural multilayer skeletal muscles. Therefore, multiple attempts should be undertaken to engineer 3D aligned structures fabricating aligned 3D skeletal muscle fiber bundles. Recently, the 4D biofabrication technique is introduced to produce multilayer scroll-like tubular constructs via programmed shape transformation [143]. Besides, scaffolds for muscle tissue engineering must facilitate further maturation of myotubes, such as electrical conductivity and contractility. Therefore, chemical modifications or conductive materials should be combined with the topographical cues for promoting myotube formation. Comparing to structure bionics, function bionics can combine more organically with the host, as the future direction of efforts. In addition, neuronal and vascular input is essential for muscle development and function. For example, the absence of a vascular network would limit the size of the scaffold. Hence, how to establish a biomimetic vascular network and innervation is challenging, which would provide a research basis for the clinical application of large biomimetic muscle scaffolds.

Tendon tissue engineering

The brief introduction to tendon

The tendon is a kind of dense connective tissue that connects bones and muscles. It can transmit the force of muscle contraction to the bone, and guide bone movement. Natural tendons are soft elastic fiber tissues, composed of its basic structural units—collagen fibers and a small number of tendon cells, with a highly oriented structure [144]. The tendon cells are arranged in parallel between collagen fiber bundles. Furthermore, it is generally believed that the arrangement of collagen fibers is parallel to the direction of the force, but some fiber bundles are twisted or staggered to prevent the fibers from separating and at the same time help to buffer forces from different directions. Although the tendon itself cannot contract, it can resist a lot of tension in virtue of the highly oriented structures.

The applications of aligned structures

Scaffolds can be used to repair tendons, injuries of which are common and painful [145]. However, tendons regenerate poorly because of low cellularity and vascularity [146]. The principal therapies (conservative management and surgical intervention) are often ineffective [147]. Tissue-engineered tendon repair is attracting attention [148, 149]. An ideal scaffold should promote cell alignment and differentiation along the tendon and ECM production. Well-aligned nanofibers [150, 151] have been shown to improve cell orientation, differentiation toward the tenogenic lineage, tendon-related gene expression, and mechanical properties in vitro. In an in vivo model of Achilles tendon repair, aligned fibrous scaffolds not only recruit host cells and enhance tenogenic gene expression but also facilitate the formation of parallel-aligned collagen fibers and tendon-like tissue [152, 153]. Orr et al. fabricated a novel scaffold for rotator cuff tendon tissue engineering, combining a multilayered electrospinning technique with a hybrid of several electrospinning alignment techniques [154]. The real-time quantitative reverse transcription–polymerase chain reaction is used to explore tendon-related gene expression, and Picrosirius Red staining under polarized light is employed to detect human type I and III collagens. Aligned, multilayered electrospun scaffolds enhance TNMD and COL3A1 expression and the formation of collagen fibrils that are more aligned than those associated with nonaligned multilayered scaffolds. Collagen-glycosaminoglycan (CG) scaffolds fabricated via lyophilization promote tendon cell proliferation and alignment and improve tendon regenerative capacity. The longitudinally aligned microstructures of CG scaffolds serve as contact guidance cues [52]. Given the major limitation of electrospun nanofibrous scaffolds (the compact structure inhibits cell infiltration), several groups have fabricated novel nanofibrous scaffolds based on electrospun nanofiber yarns including yarn-based woven bio-textiles [155], nanoyarn networks [156], and electrospun-aligned, nanoyarn-reinforced nanofibrous scaffolds [157]. As shown in Fig. 5bi, Wu et al. fabricated nanofibrous woven textiles (PCL nanofiber yarns) for tendon regeneration [155]. The structure and nanoscale organization of the materials are similar to those of native tendon ECM. And as compared to electrospun random and aligned meshes, the test results of Young's moduli and ultimate tensile strengths demonstrate that the woven fabrics have better mechanical characteristics (Fig. 5bii). Meanwhile, given the 3D-aligned microstructure and large pore size, nanofibrous woven textiles could promote cell viability, orientation, infiltration, and tendon gene expression. For example, the aligned fibers of woven fabrics and electrospun aligned meshes promote TNMD and COL1 protein formation along the fiber direction, mimicking the ECM architecture of the native tendon (Fig. 5biii).

Perspectives and outlook about tendon regeneration

Overall, well-aligned nanofibers have many inherent benefits in tendon tissue repair. The main reason is that they are similar to the collagen fibrils matrix in the native tendon. Meanwhile, many properties can be adjusted, including mechanical properties, porosity, fiber diameter, and degradation rate. As such, aligned nanofiber techniques suffer from certain limitations and challenges. For example, compared with other scaffolds (such as nerve tissue engineering scaffold), the tendon tissue engineering scaffold needs to suffer higher elasticity and tensile strength. Therefore, the post-processing of electro-

spinning fibers (such as forming nanofibrous woven textiles) becomes a common method, which can enhance the mechanical properties to meet the needs of tendon repair. However, most of the time, the increase in mechanical properties would decrease the degradation rate. It may impact on the efficiency of tendon repair. Therefore, how to balance mechanical properties and degradation rate should be attended to. In addition, the tendon tissue also has thick multilayer structures, which is the foundation of function. It is difficult for current electrospinning technology to fabricate thick multilayer structures, but even if it can, the process is complicated at a high cost and low efficiency. Hence, the electrospinning technology would be improved, such as the improvement of the 3D collector device, the combination with other fabrication, and so on. Meanwhile, to promote the tendon in function, how to simulate the 3D tension environment of the natural tendon also needs to be addressed.

Dentin tissue engineering

Dentin is a major tooth component consisting of millions of tubules (15,000–48,000/mm^2) of diameter 2–4 μm [158]. The dentin ECM is nanofibrous at the nanoscale level. It is difficult to impart tubular micropatterns to nanofibrous structures using routine methods such as microcontact printing. As shown in Fig. 5ci, Ma et al. combined unique, maskless, laser-guided micropatterning and electrospinning to create a 3D nanofibrous tubular matrix with the hierarchical architecture of natural dentin ECM [94]. The technique features non-contact, high-precision, flexible computer programming of machining. First, a nanofibrous gelatin matrix is produced and cross-linked via electrospinning. Next, a tubular micropattern is created within the matrix using a Leica laser microdissector (Model 7000; Leica, Germany). The size and depth of the tubular pores and the distance between tubules can be adjusted by changing the laser parameters. The size and pattern of tubules within the 3D nanofibrous tubular matrix are the same as those of natural dentin ECM. Odontoblasts seeded onto the micropatterned matrix align with the pore surfaces and secret many collagen fibers oriented along the tubules; cells cultured on a non-micropatterned matrix do not. The matrix promotes the differentiation of dental pulp stem cells into odontoblasts, as revealed by the expression of differentiation genes including ALP, Col I, and DSPP (Fig. 5cii). Besides, the Masson's trichrome staining and SEM results of cell/nanofibrous tubular gelatin matrix constructs in nude mice demonstrates that the tubular gelatin scaffold could promote regeneration of the tubular and vascularized pulpodentin complex (Fig. 5ciii). Such tubular structures would aid the regeneration of other tubular tissues such as blood vessels.

Conclusions and future perspectives

Cells are often aligned in an organized manner in tissues such as muscles, vascular tissue, and nerves. This affords a normal structure and maintains tissue function. Many aligned structures that guide cell orientation have been used in tissue engineering, including aligned electrospun nanofibers, porous or channeled structures, micropatterns, and combinations thereof. These allow functional recovery and tissue regeneration. However, challenges remain. First, the molecular mechanism underlying cell alignment organization requires study, as do the interactions (especially long term) between engineered products and the host. This would enhance the efficiency and stability of engineered structures. Second, most existing aligned structures are 2D, thus dramatically differ from the 3D cellular environment. Cells behave differently in 3D and 2D constructs. Currently, we can guide early cell growth but cannot biofabricate the complex 3D micro-architectures essential for tissue maturation in vivo. Existing structures are poorly functional. The biofabrication of complex, 3D aligned micro-architectures within scaffolds is challenging. Finally, although many aligned structures are available, most studies focused on single scaffold structures, limiting the efficiency and accuracy of cellular orientation. In the future, various aligned structures should be combined (for example, the aligned nanofibers and micropatterns mentioned above). Also, other cues (biological signals and mechanical loadings) that control cellular orientation should be considered. Given the remarkable advances in cell biology and biomaterials science and engineering, the challenges will be met.

Acknowledgements This work was financially supported by the National Key Research and Development Program of China (2018YFA0703000), the National Natural Science Foundation of China (81670972, 31872752), Key Research and Development Program of Zhejiang, China (2017C01054, 2018C03062, 2017C01063), and Postdoctoral Science Foundation of China (2020TQ0257, 2020M681896).

Author contributions KL, YQ, MY and HW designed the research and drafted the manuscript. JG and ZZ helped organize the manuscript. KL, JG, YQ, ZZ, JY, LM, MY and HW revised and finalized the paper. All authors have read and approved the final manuscript and, therefore, have full access to all the data in the study and take responsibility for the integrity and security of the data.

Compliance with ethical standards

Conflict of interest The authors declare that they have no conflict of interest.

Ethical approval This article does not contain any studies with human or animal subjects performed by any of the authors.

References

1. Morimoto Y, Takeuchi S (2017) In vitro construction of skeletal muscle tissues. Clin Calcium 27(3):383–389
2. Serbo JV, Gerecht S (2013) Vascular tissue engineering: biodegradable scaffold platforms to promote angiogenesis. Stem Cell Res Ther 4(1):8. https://doi.org/10.1186/scrt156
3. Thompson DM, Buettner HM (2006) Neurite outgrowth is directed by Schwann cell alignment in the absence of other guidance cues. Ann Biomed Eng 34(4):669–676. https://doi.org/10.1007/s10439-005-9053-9
4. Yang GH, Lee J, Kim G (2019) The fabrication of uniaxially aligned micro-textured polycaprolactone struts and application for skeletal muscle tissue regeneration. Biofabrication 11:025005. https://doi.org/10.1088/1758-5090/ab0098
5. Llopis-Grimalt MA, Amengual-Tugores AM, Monjo M, Ramis JM (2019) Oriented cell alignment induced by a nanostructured titanium surface enhances expression of cell differentiation markers. Nanomaterials 9(12):1661. https://doi.org/10.3390/nano9121661
6. Khademhosseini A, Langer R (2016) A decade of progress in tissue engineering. Nat Protoc 11(10):1775–1781. https://doi.org/10.1038/nprot.2016.123
7. Guven S, Chen P, Inci F, Tasoglu S, Erkmen B, Demirci U (2015) Multiscale assembly for tissue engineering and regenerative medicine. Trends Biotechnol 33(5):269–279. https://doi.org/10.1016/j.tibtech.2015.02.003
8. Xing F, Li L, Zhou C, Long C, Wu L, Lei H, Kong Q, Fan Y, Xiang Z, Zhang X (2019) Regulation and directing stem cell fate by tissue engineering functional microenvironments: scaffold physical and chemical cues. Stem Cells Int 2019:2180925. https://doi.org/10.1155/2019/2180925
9. Xia H, Chen Q, Fang Y, Liu D, Zhong D, Wu H, Xia Y, Yan Y, Tang W, Sun X (2014) Directed neurite growth of rat dorsal root ganglion neurons and increased colocalization with Schwann cells on aligned poly(methyl methacrylate) electrospun nanofibers. Brain Res 1565:18–27. https://doi.org/10.1016/j.brainres.2014.04.002
10. Metavarayuth K, Sitasuwan P, Zhao X, Lin Y, Wang Q (2016) Influence of surface topographical cues on the differentiation of mesenchymal stem cells in vitro. ACS Biomater Sci Eng 2(2):142–151. https://doi.org/10.1021/acsbiomaterials.5b00377
11. Li GC, Zhao XY, Zhang LZ, Wang CP, Shi YW, Yang YM (2014) Regulating Schwann cells growth by chitosan micropatterning for peripheral nerve regeneration in vitro. Macromol Biosci 14(8):1067–1075. https://doi.org/10.1002/mabi.201400098
12. Pan F, Zhang M, Wu G, Lai Y, Greber B, Scholer HR, Chi L (2013) Topographic effect on human induced pluripotent stem cells differentiation towards neuronal lineage. Biomaterials 34(33):8131–8139. https://doi.org/10.1016/j.biomaterials.2013.07.025
13. Silva M, Ferreira FN, Alves NM, Paiva MC (2020) Biodegradable polymer nanocomposites for ligament/tendon tissue engineering. J Nanobiotechnol 18(1):23. https://doi.org/10.1186/s12951-019-0556-1
14. Staples RJ, Ivanovski S, Vaquette C (2020) Fibre guiding scaffolds for periodontal tissue engineering. J Periodontal Res 55(3):331–341. https://doi.org/10.1111/jre.12729
15. Shi Y, Li Y, Coradin T (2020) Magnetically-oriented type I collagen-SiO_2@Fe_3O_4 rods composite hydrogels tuning skin cell growth. Colloids Surf B Biointerfaces 185:110597. https://doi.org/10.1016/j.colsurfb.2019.110597
16. Gong HY, Park J, Kim W, Kim J, Lee JY, Koh WG (2019) A Novel Conductive and Micropatterned PEG-Based Hydrogel Enabling the Topographical and Electrical Stimulation of Myoblasts. ACS Appl Mater Interfaces 11(51):47695–47706. https://doi.org/10.1021/acsami.9b16005
17. Patel M, Min JH, Hong MH, Lee HJ, Kang S, Yi S, Koh WG (2020) Culture of neural stem cells on the conductive and microgrooved polymeric scaffolds fabricated via electrospun fiber-template lithography (EFTL). Biomed Mater 15(4):045007. https://doi.org/10.1088/1748-605X/ab763b
18. Kim JI, Kim CS, Park CH (2018) Harnessing nanotopography of electrospun nanofibrous nerve guide conduits (NGCs) for neural tissue engineering. Adv Exp Med Biol 1078:395–408. https://doi.org/10.1007/978-981-13-0950-2_20
19. Jin G, He R, Sha B, Li W, Qing H, Teng R, Xu F (2018) Electrospun three-dimensional aligned nanofibrous scaffolds for tissue engineering. Mater Sci Eng C Mater Biol Appl 92:995–1005. https://doi.org/10.1016/j.msec.2018.06.065
20. Jiang T, Carbone EJ, Lo KWH, Laurencin CT (2015) Electrospinning of polymer nanofibers for tissue regeneration. Prog Polym Sci 46:1–24. https://doi.org/10.1016/j.progpolymsci.2014.12.001
21. Ren YJ, Zhang S, Mi R, Liu Q, Zeng X, Rao M, Hoke A, Mao HQ (2013) Enhanced differentiation of human neural crest stem cells towards the Schwann cell lineage by aligned electrospun fiber matrix. Acta Biomater 9(8):7727–7736. https://doi.org/10.1016/j.actbio.2013.04.034
22. Li X, Wang X, Yao D, Jiang J, Guo X, Gao Y, Li Q, Shen C (2018) Effects of aligned and random fibers with different diameter on cell behaviors. Colloids Surf B Biointerfaces 171:461–467. https://doi.org/10.1016/j.colsurfb.2018.07.045
23. Ingavle GC, Leach JK (2014) Advancements in electrospinning of polymeric nanofibrous scaffolds for tissue engineering. Tissue Eng Part B Rev 20(4):277–293. https://doi.org/10.1089/ten.TEB.2013.0276
24. Taylor GI (1964) Disintegration of water drops in an electric field. Proc R Soc Lond A 280(1382):383–397
25. Xue J, Xie J, Liu W, Xia Y (2017) Electrospun nanofibers: new concepts, materials, and applications. Acc Chem Res 50(8):1976–1987. https://doi.org/10.1021/acs.accounts.7b00218
26. Hunley MT, Long TE (2008) Electrospinning functional nanoscale fibers: a perspective for the future. Polym Int 57(3):385–389. https://doi.org/10.1002/pi.2320
27. Kenry LC (2017) Nanofiber technology: current status and emerging developments. Prog Polym Sci 70:1–17. https://doi.org/10.1016/j.progpolymsci.2017.03.002
28. Sun B, Long YZ, Zhang HD, Li MM, Duvail JL, Jiang XY, Yin HL (2014) Advances in three-dimensional nanofibrous macrostructures via electrospinning. Prog Polym Sci 39(5):862–890. https://doi.org/10.1016/j.progpolymsci.2013.06.002
29. Li D, Wang YL, Xia YN (2003) Electrospinning of polymeric and ceramic nanofibers as uniaxially aligned arrays. Nano Lett 3(8):1167–1171. https://doi.org/10.1021/nl0344256
30. Shalumon KT, Sathish D, Nair SV, Chennazhi KP, Tamura H, Jayakumar R (2012) Fabrication of aligned poly(lactic acid)-chitosan nanofibers by novel parallel blade collector method for skin tissue engineering. J Biomed Nanotechnol 8(3):405–416. https://doi.org/10.1166/jbn.2012.1395
31. Yang D, Lu B, Zhao Y, Jiang X (2007) Fabrication of aligned fibrous arrays by magnetic electrospinning. Adv Mater 19(21):3702–3706
32. Chen MC, Sun YC, Chen YH (2013) Electrically conductive nanofibers with highly oriented structures and their potential application in skeletal muscle tissue engineering. Acta Biomater 9(3):5562–5572. https://doi.org/10.1016/j.actbio.2012.10.024
33. Sun B, Jiang XJ, Zhang S, Zhang JC, Li YF, You QZ, Long YZ (2015) Electrospun anisotropic architectures and porous structures for tissue engineering. J Mater Chem B 3(27):5389–5410. https://doi.org/10.1039/c5tb00472a

34. Abudula T, Saeed U, Salah N, Memic A, Al-Turaif H (2018) Study of electrospinning parameters and collection methods on size distribution and orientation of PLA/PBS hybrid fiber using digital image processing. J Nanosci Nanotechnol 18(12):8240–8251. https://doi.org/10.1166/jnn.2018.15885
35. Xu CY, Inai R, Kotaki M, Ramakrishna S (2004) Aligned biodegradable nanofibrous structure: a potential scaffold for blood vessel engineering. Biomaterials 25(5):877–886. https://doi.org/10.1016/s0142-9612(03)00593-3
36. Katta P, Alessandro M, Ramsier RD, Chase GG (2004) Continuous electrospinning of aligned polymer nanofibers onto a wire drum collector. Nano Lett 4(11):2215–2218. https://doi.org/10.1021/nl0486158
37. Wu HJ, Hu MH, Tuan-Mu HY, Hu JJ (2019) Preparation of aligned poly(glycerol sebacate) fibrous membranes for anisotropic tissue engineering. Mater Sci Eng C Mater Biol Appl 100:30–37. https://doi.org/10.1016/j.msec.2019.02.098
38. Alazab M, Mitchell GR, Davis FJ, Mohan SD (2017) Sustainable electrospinning of nanoscale fibres. Procedia Manuf 12:66–78. https://doi.org/10.1016/j.promfg.2017.08.009
39. Nitti P, Gallo N, Natta L, Scalera F, Palazzo B, Sannino A, Gervaso F (2018) Influence of nanofiber orientation on morphological and mechanical properties of electrospun chitosan mats. J Healthc Eng 2018:3651480. https://doi.org/10.1155/2018/3651480
40. Jana S, Levengood SK, Zhang M (2016) Anisotropic materials for skeletal-muscle-tissue engineering. Adv Mater 28(48):10588–10612. https://doi.org/10.1002/adma.201600240
41. Teo WE, Kotaki M, Mo XM, Ramakrishna S (2005) Porous tubular structures with controlled fibre orientation using a modified electrospinning method. Nanotechnology 16(6):918–924. https://doi.org/10.1088/0957-4484/16/6/049
42. Jana S, Zhang M (2013) Fabrication of 3D aligned nanofibrous tubes by direct electrospinning. J Mater Chem B 1(20):2575–2581. https://doi.org/10.1039/c3tb20197j
43. Liu SL, Long YZ, Zhang ZH, Zhang HD, Sun B, Zhang JC, Han WP (2013) Assembly of oriented ultrafine polymer fibers by centrifugal electrospinning. J Nanomater 2013:713275. https://doi.org/10.1155/2013/713275
44. Khamforoush M, Asgari T, Hatami T, Dabirian F (2014) The influences of collector diameter, spinneret rotational speed, voltage, and polymer concentration on the degree of nanofibers alignment generated by electrocentrifugal spinning method: modeling and optimization by response surface methodology. Korean J Chem Eng 31(9):1695–1706. https://doi.org/10.1007/s11814-014-0099-y
45. Edmondson D, Cooper A, Jana S, Wood D, Zhang MQ (2012) Centrifugal electrospinning of highly aligned polymer nanofibers over a large area. J Mater Chem 22(35):18646–18652. https://doi.org/10.1039/c2jm33877g
46. Erickson AE, Edmondson D, Chang FC, Wood D, Gong A, Levengood SL, Zhang M (2015) High-throughput and high-yield fabrication of uniaxially-aligned chitosan-based nanofibers by centrifugal electrospinning. Carbohydr Polym 134:467–474. https://doi.org/10.1016/j.carbpol.2015.07.097
47. Xie JW, MacEwan MR, Ray WZ, Liu WY, Siewe DY, Xia YN (2010) Radially aligned, electrospun nanofibers as dural substitutes for wound closure and tissue regeneration applications. ACS Nano 4(9):5027–5036. https://doi.org/10.1021/nn101554u
48. Stocco TD, Rodrigues BVM, Marciano FR, Lobo AO (2017) Design of a novel electrospinning setup for the fabrication of biomimetic scaffolds for meniscus tissue engineering applications. Mater Lett 196:221–224. https://doi.org/10.1016/j.matlet.2017.03.055
49. Kim JI, Kim JY, Park CH (2018) Fabrication of transparent hemispherical 3D nanofibrous scaffolds with radially aligned patterns via a novel electrospinning method. Sci Rep 8(1):3424. https://doi.org/10.1038/s41598-018-21618-0
50. Francis NL, Hunger PM, Donius AE, Riblett BW, Zavaliangos A, Wegst UG, Wheatley MA (2013) An ice-templated, linearly aligned chitosan-alginate scaffold for neural tissue engineering. J Biomed Mater Res A 101(12):3493–3503. https://doi.org/10.1002/jbm.a.34668
51. Zhang Q, Zhao Y, Yan S, Yang Y, Zhao H, Li M, Lu S, Kaplan DL (2012) Preparation of uniaxial multichannel silk fibroin scaffolds for guiding primary neurons. Acta Biomater 8(7):2628–2638. https://doi.org/10.1016/j.actbio.2012.03.033
52. Caliari SR, Harley BA (2011) The effect of anisotropic collagen-GAG scaffolds and growth factor supplementation on tendon cell recruitment, alignment, and metabolic activity. Biomaterials 32(23):5330–5340. https://doi.org/10.1016/j.biomaterials.2011.04.021
53. Neffe AT, Pierce BF, Tronci G, Ma N, Pittermann E, Gebauer T, Frank O, Schossig M, Xu X, Willie BM, Forner M, Ellinghaus A, Lienau J, Duda GN, Lendlein A (2015) One step creation of multifunctional 3D architectured hydrogels inducing bone regeneration. Adv Mater 27(10):1738–1744. https://doi.org/10.1002/adma.201404787
54. Davidenko N, Gibb T, Schuster C, Best SM, Campbell JJ, Watson CJ, Cameron RE (2012) Biomimetic collagen scaffolds with anisotropic pore architecture. Acta Biomater 8(2):667–676. https://doi.org/10.1016/j.actbio.2011.09.033
55. Zhu JT, Wang JW, Liu QY, Liu YH, Wang L, He CC, Wang HL (2013) Anisotropic tough poly(2-hydroxyethyl methacrylate) hydrogels fabricated by directional freezing redox polymerization. J Mater Chem B 1(7):978–986. https://doi.org/10.1039/c2tb00288d
56. Barg S, Perez FM, Ni N, Pereira PDV, Maher RC, Garcia-Tunn E, Eslava S, Agnoli S, Mattevi C, Saiz E (2014) Mesoscale assembly of chemically modified graphene into complex cellular networks. Nat Commun. https://doi.org/10.1038/ncomms5328
57. Delattre B, Bai H, Ritchie RO, De Coninck J, Tomsia AP (2014) Unidirectional freezing of ceramic suspensions: in situ X-ray investigation of the effects of additives. ACS Appl Mater Interfaces 6(1):159–166. https://doi.org/10.1021/am403793x
58. Panseri S, Montesi M, Dozio SM, Savini E, Tampieri A, Sandri M (2016) Biomimetic scaffold with aligned microporosity designed for dentin regeneration. Front Bioeng Biotechnol 4:48. https://doi.org/10.3389/fbioe.2016.00048
59. Porter MM, Yeh M, Strawson J, Goehring T, Lujan S, Siripasopsotorn P, Meyers MA, McKittrick J (2012) Magnetic freeze casting inspired by nature. Mat Sci Eng A Struct 556:741–750. https://doi.org/10.1016/j.msea.2012.07.058
60. Porter MM, Niksiar P, McKittrick J (2016) Microstructural control of colloidal-based ceramics by directional solidification under weak magnetic fields. J Am Ceram Soc 99(6):1917–1926. https://doi.org/10.1111/jace.14183
61. Nelson I, Ogden TA, Al Khateeb S, Graser J, Sparks TD, Abbott JJ, Naleway SE (2019) Freeze-casting of surface-magnetized iron(II, III) oxide particles in a uniform static magnetic field generated by a Helmholtz coil. Adv Eng Mater 21(3):1801092
62. Nelson I, Gardner L, Carlson K, Naleway SE (2019) Freeze casting of iron oxide subject to a tri-axial nested Helmholtz-coils driven uniform magnetic field for tailored porous scaffolds. Acta Mater 173:106–116. https://doi.org/10.1016/j.actamat.2019.05.003
63. Zhang YM, Hu LY, Han JC (2009) Preparation of a dense/porous bilayered ceramic by applying an electric field during freeze casting. J Am Ceram Soc 92(8):1874–1876. https://doi.org/10.1111/j.1551-2916.2009.03110.x
64. Tang YF, Zhao K, Wei JQ, Qin YS (2010) Fabrication of aligned lamellar porous alumina using directional solidification of aque-

ous slurries with an applied electrostatic field. J Eur Ceram Soc 30(9):1963–1965. https://doi.org/10.1016/j.jeurceramsoc.2010.03.012
65. Tang YF, Qiu S, Miao Q, Wu C (2016) Fabrication of lamellar porous alumina with axisymmetric structure by directional solidification with applied electric and magnetic fields. J Eur Ceram Soc 36(5):1233–1240. https://doi.org/10.1016/j.jeurceramsoc.2015.12.012
66. Bai H, Chen Y, Delattre B, Tomsia AP, Ritchie RO (2015) Bioinspired large-scale aligned porous materials assembled with dual temperature gradients. Sci Adv 1(11):e1500849. https://doi.org/10.1126/sciadv.1500849
67. Bai H, Wang D, Delattre B, Gao W, De Coninck J, Li S, Tomsia AP (2015) Biomimetic gradient scaffold from ice-templating for self-seeding of cells with capillary effect. Acta Biomater 20:113–119. https://doi.org/10.1016/j.actbio.2015.04.007
68. Tang YF, Miao Q, Qiu S, Zhao K, Hu L (2014) Novel freeze-casting fabrication of aligned lamellar porous alumina with a centrosymmetric structure. J Eur Ceram Soc 34(15):4077–4082. https://doi.org/10.1016/j.jeurceramsoc.2014.05.040
69. Fan L, Li JL, Cai Z, Wang X (2018) Creating biomimetic anisotropic architectures with co-aligned nanofibers and macrochannels by manipulating ice crystallization. ACS Nano 12(6):5780–5790. https://doi.org/10.1021/acsnano.8b01648
70. Shao G, Hanaor DAH, Shen X, Gurlo A (2020) Freeze casting: from low-dimensional building blocks to aligned porous structures—a review of novel materials, methods, and applications. Adv Mater 32(17):e1907176. https://doi.org/10.1002/adma.201907176
71. Du W, Hong S, Scapin G, Goulard M, Shah DI (2019) Directed Collective Cell Migration Using Three-Dimensional Bioprinted Micropatterns on Thermoresponsive Surfaces for Myotube Formation. Acs Biomater Sci Eng 5(8):3935–3943. https://doi.org/10.1021/acsbiomaterials.8b01359
72. Li D, Wang YL (2018) Coordination of cell migration mediated by site-dependent cell-cell contact. Proc Natl Acad Sci USA 115(42):10678–10683. https://doi.org/10.1073/pnas.1807543115
73. Kim SE, Kim MS, Shin YC, Eom SU, Lee JH, Shin DM, Hong SW, Kim B, Park JC, Shin BS, Lim D, Han DW (2016) Cell migration according to shape of graphene oxide micropatterns. Micromachines (Basel). https://doi.org/10.3390/mi7100186
74. Paul CD, Hung WC, Wirtz D, Konstantopoulos K (2016) Engineered models of confined cell migration. Annu Rev Biomed Eng 18:159–180. https://doi.org/10.1146/annurev-bioeng-071114-040654
75. Yoon SH, Kim YK, Han ED, Seo YH, Kim BH, Mofrad MRK (2012) Passive control of cell locomotion using micropatterns: the effect of micropattern geometry on the migratory behavior of adherent cells. Lab Chip 12(13):2391–2402. https://doi.org/10.1039/c2lc40084g
76. Dahl KN, Ribeiro AJ, Lammerding J (2008) Nuclear shape, mechanics, and mechanotransduction. Circ Res 102(11):1307–1318. https://doi.org/10.1161/CIRCRESAHA.108.173989
77. Ermis M, Akkaynak D, Chen P, Demirci U, Hasirci V (2016) A high throughput approach for analysis of cell nuclear deformability at single cell level. Sci Rep 6:36917. https://doi.org/10.1038/srep36917
78. Peng R, Yao X, Ding J (2011) Effect of cell anisotropy on differentiation of stem cells on micropatterned surfaces through the controlled single cell adhesion. Biomaterials 32(32):8048–8057. https://doi.org/10.1016/j.biomaterials.2011.07.035
79. Yap FL, Zhang Y (2007) Protein and cell micropatterning and its integration with micro/nanoparticles assembly. Biosens Bioelectron 22(6):775–788. https://doi.org/10.1016/j.bios.2006.03.016
80. Lin XX, Shi Y, Cao YL, Liu W (2016) Recent progress in stem cell differentiation directed by material and mechanical cues. Biomed Mater 11(1):014109. https://doi.org/10.1088/1748-6041/11/1/014109
81. Saner CK, Lu L, Zhang DH, Garno JC (2015) Chemical approaches for nanoscale patterning based on particle lithography with proteins and organic thin films. Nanotechnol Rev 4(2):129–143. https://doi.org/10.1515/ntrev-2015-0002
82. Ermis M, Antmen E, Hasirci V (2018) Micro and nanofabrication methods to control cell-substrate interactions and cell behavior: a review from the tissue engineering perspective. Bioact Mater 3(3):355–369. https://doi.org/10.1016/j.bioactmat.2018.05.005
83. D'Arcangelo E, McGuigan AP (2015) Micropatterning strategies to engineer controlled cell and tissue architecture in vitro. Biotechniques 58(1):13–23. https://doi.org/10.2144/000114245
84. Chen G, Kawazoe N (2020) Regulation of stem cell functions by micro-patterned structures. Adv Exp Med Biol 1250:141–155. https://doi.org/10.1007/978-981-15-3262-7_10
85. Sen AK, Raj A, Banerjee U, Iqbal SR (2019) Soft lithography, molding, and micromachining techniques for polymer micro devices. Methods Mol Biol 1906:13–54. https://doi.org/10.1007/978-1-4939-8964-5_2
86. Perl A, Reinhoudt DN, Huskens J (2009) Microcontact printing: limitations and achievements. Adv Mater 21(22):2257–2268. https://doi.org/10.1002/adma.200801864
87. Park TH, Shuler ML (2003) Integration of cell culture and microfabrication technology. Biotechnol Prog 19(2):243–253. https://doi.org/10.1021/bp020143k
88. Friguglietti J, Das S, Le P, Fraga D, Quintela M, Gazze SA, McPhail D, Gu J, Sabek O, Gaber AO, Francis LW, Zagozdzon-Wosik W, Merchant FA (2020) Novel silicon titanium diboride micropatterned substrates for cellular patterning. Biomaterials 244:119927. https://doi.org/10.1016/j.biomaterials.2020.119927
89. Macadangdang J, Lee HJ, Carson D, Jiao A, Fugate J, Pabon L, Regnier M, Murry C, Kim DH (2014) Capillary force lithography for cardiac tissue engineering. J Vis Exp (88):50039. https://doi.org/10.3791/50039
90. Lee MR, Kwon KW, Jung H, Kim HN, Suh KY, Kim K, Kim KS (2010) Direct differentiation of human embryonic stem cells into selective neurons on nanoscale ridge/groove pattern arrays. Biomaterials 31(15):4360–4366. https://doi.org/10.1016/j.biomaterials.2010.02.012
91. Jeong HE, Kwak R, Kim JK, Suh KY (2008) Generation and self-replication of monolithic, dual-scale polymer structures by two-step capillary-force lithography. Small 4(11):1913–1918. https://doi.org/10.1002/smll.200800151
92. Li JY, Ho YC, Chung YC, Lin FC, Liao WL, Tsai WB (2013) Preparation of micron/submicron hybrid patterns via a two-stage UV-imprint technique and their dimensional effects on cell adhesion and alignment. Biofabrication 5(3):035003. https://doi.org/10.1088/1758-5082/5/3/035003
93. Lu JY, Zhang XX, Zhu QY, Zhang FR, Huang WT, Ding XZ, Xia LQ, Luo HQ, Li NB (2018) Highly tunable and scalable fabrication of 3D flexible graphene micropatterns for directing cell alignment. ACS Appl Mater Interfaces 10(21):17704–17713. https://doi.org/10.1021/acsami.8b04416
94. Ma C, Qu TJ, Chang B, Jing Y, Feng JQ, Liu XH (2018) 3D maskless micropatterning for regeneration of highly organized tubular tissues. Adv Healthc Mater 7(3):1700738. https://doi.org/10.1002/adhm.201700738
95. Park JA, Yoon S, Kwon J, Now H, Kim YK, Kim WJ, Yoo JY, Jung S (2018) Freeform micropatterning of living cells into cell culture medium using direct inkjet printing. Sci Rep 7:1–11

96. Sumaru K, Takagi T, Morishita K, Satoh T, Kanamori T (2018) Fabrication of pocket-like hydrogel microstructures through photolithography. Soft Matter 14(28):5710–5714. https://doi.org/10.1039/c8sm00865e
97. Gantumur E, Kimura M, Taya M, Horie M, Nakamura M, Sakai S (2020) Inkjet micropatterning through horseradish peroxidase-mediated hydrogelation for controlled cell immobilization and microtissue fabrication. Biofabrication 12(1):011001. https://doi.org/10.1088/1758-5090/ab3b3c
98. Cha SH, Lee HJ, Koh WG (2017) Study of myoblast differentiation using multi-dimensional scaffolds consisting of nano and micropatterns. Biomater Res 21(1):1. https://doi.org/10.1186/s40824-016-0087-x
99. Li H, Wen F, Chen H, Pal M, Lai Y, Zhao AZ, Tan LP (2016) Micropatterning extracellular matrix proteins on electrospun fibrous substrate promote human mesenchymal stem cell differentiation toward neurogenic lineage. ACS Appl Mater Interfaces 8(1):563–573. https://doi.org/10.1021/acsami.5b09588
100. Shi J, Wang L, Chen Y (2009) Microcontact printing and lithographic patterning of electrospun nanofibers. Langmuir 25(11):6015–6018. https://doi.org/10.1021/la900811k
101. Stevens MM, George JH (2005) Exploring and engineering the cell surface interface. Science 310(5751):1135–1138. https://doi.org/10.1126/science.1106587
102. Huang C, Tang YW, Liu X, Sutti A, Ke QF, Mo XM, Wang XG, Morsi Y, Lin T (2011) Electrospinning of nanofibres with parallel line surface texture for improvement of nerve cell growth. Soft Matter 7(22):10812–10817. https://doi.org/10.1039/c1sm06430d
103. Sharma CS, Sharma A, Madou M (2010) Multiscale carbon structures fabricated by direct micropatterning of electrospun mats of SU-8 photoresist nanofibers. Langmuir 26(4):2218–2222. https://doi.org/10.1021/la904078r
104. Sankar S, Kakunuri M, Eswaramoorthy SD, Sharma CS, Rath SN (2018) Effect of patterned electrospun hierarchical structures on alignment and differentiation of mesenchymal stem cells: biomimicking bone. J Tissue Eng Regen Med 12(4):E2073–E2084. https://doi.org/10.1002/term.2640
105. Zhang LZ, Chen SY, Liang RY, Chen Y, Li SJ, Li SQ, Sun ZD, Wang YL, Li GC, Ming AJ, Yang YM (2018) Fabrication of alignment polycaprolactone scaffolds by combining use of electrospinning and micromolding for regulating Schwann cells behavior. J Biomed Mater Res A 106(12):3123–3134. https://doi.org/10.1002/jbm.a.36507
106. Guex AG, Birrer DL, Fortunato G, Tevaearai HT, Giraud MN (2013) Anisotropically oriented electrospun matrices with an imprinted periodic micropattern: a new scaffold for engineered muscle constructs. Biomed Mater. https://doi.org/10.1088/1748-6041/8/2/021001
107. Ma J, He Y, Liu X, Chen W, Wang A, Lin CY, Mo X, Ye X (2018) A novel electrospun-aligned nanoyarn/three-dimensional porous nanofibrous hybrid scaffold for annulus fibrosus tissue engineering. Int J Nanomed 13:1553–1567. https://doi.org/10.2147/IJN.S143990
108. Jin G, Li J, Li K (2017) Photosensitive semiconducting polymer-incorporated nanofibers for promoting the regeneration of skin wound. Mater Sci Eng C Mater Biol Appl 70(Pt 2):1176–1181. https://doi.org/10.1016/j.msec.2016.04.107
109. Montero RB, Vial X, Nguyen DT, Farhand S, Reardon M, Pham SM, Tsechpenakis G, Andreopoulos FM (2012) bFGF-containing electrospun gelatin scaffolds with controlled nano-architectural features for directed angiogenesis. Acta Biomater 8(5):1778–1791. https://doi.org/10.1016/j.actbio.2011.12.008
110. Park S, Kim D, Park S, Kim S, Lee D, Kim W, Kim J (2018) Nanopatterned scaffolds for neural tissue engineering and regenerative medicine. Adv Exp Med Biol 1078:421–443. https://doi.org/10.1007/978-981-13-0950-2_22
111. Chiono V, Tonda-Turo C (2015) Trends in the design of nerve guidance channels in peripheral nerve tissue engineering. Prog Neurobiol 131:87–104. https://doi.org/10.1016/j.pneurobio.2015.06.001
112. Carvalho CR, Oliveira JM, Reis RL (2019) Modern trends for peripheral nerve repair and regeneration: beyond the hollow nerve guidance conduit. Front Bioeng Biotechnol 7:337. https://doi.org/10.3389/fbioe.2019.00337
113. Samadian H, Ehterami A, Sarrafzadeh A, Khastar H, Nikbakht M, Rezaei A, Chegini L, Salehi M (2020) Sophisticated polycaprolactone/gelatin nanofibrous nerve guided conduit containing platelet-rich plasma and citicoline for peripheral nerve regeneration: in vitro and in vivo study. Int J Biol Macromol 150:380–388. https://doi.org/10.1016/j.ijbiomac.2020.02.102
114. Hou Y, Wang X, Zhang Z, Luo J, Cai Z, Wang Y, Li YJ (2019) Repairing transected peripheral nerve using a biomimetic nerve guidance conduit containing intraluminal sponge fillers. Adv Healthc Mater 8(21):1900913. https://doi.org/10.1002/adhm.201970082
115. Kim JI, Hwang TI, Aguilar LE, Park CH, Kim CS (2016) A controlled design of aligned and random nanofibers for 3D bi-functionalized nerve conduits fabricated via a novel electrospinning set-up. Sci Rep 6:23761. https://doi.org/10.1038/srep23761
116. Zhu YQ, Wang AJ, Patel S, Kurpinski K, Diao E, Bao X, Kwong G, Young WL, Li S (2011) Engineering bi-layer nanofibrous conduits for peripheral nerve regeneration. Tissue Eng Part C-Methods 17(7):705–715. https://doi.org/10.1089/ten.tec.2010.0565
117. Hu X, Huang J, Ye Z, Xia L, Li M, Lv B, Shen X, Luo Z (2009) A novel scaffold with longitudinally oriented microchannels promotes peripheral nerve regeneration. Tissue Eng Part A 15(11):3297–3308. https://doi.org/10.1089/ten.TEA.2009.0017
118. Zhang YG, Sheng QS, Qi FY, Hu XY, Zhao W, Wang YQ, Lan LF, Huang JH, Luo ZJ (2013) Schwann cell-seeded scaffold with longitudinally oriented micro-channels for reconstruction of sciatic nerve in rats. J Mater Sci Mater Med 24(7):1767–1780. https://doi.org/10.1007/s10856-013-4917-2
119. Huang C, Ouyang Y, Niu H, He N, Ke Q, Jin X, Li D, Fang J, Liu W, Fan C, Lin T (2015) Nerve guidance conduits from aligned nanofibers: improvement of nerve regeneration through longitudinal nanogrooves on a fiber surface. ACS Appl Mater Interfaces 7(13):7189–7196. https://doi.org/10.1021/am509227t
120. Zhang D, Yao Y, Duan Y, Yu X, Shi H, Nakkala JR, Zuo X, Hong L, Mao Z, Gao C (2020) Surface-anchored graphene oxide nanosheets on cell-scale micropatterned poly(d, l-lactide-co-caprolactone) conduits promote peripheral nerve regeneration. ACS Appl Mater Interfaces 12(7):7915–7930. https://doi.org/10.1021/acsami.9b20321
121. Gnavi S, Fornasari BE, Tonda-Turo C, Laurano R, Zanetti M, Ciardelli G, Geuna S (2015) The effect of electrospun gelatin fibers alignment on schwann cell and axon behavior and organization in the perspective of artificial nerve design. Int J Mol Sci 16(6):12925–12942. https://doi.org/10.3390/ijms160612925
122. Singh A, Shiekh PA, Das M, Seppala J, Kumar A (2019) Aligned chitosan-gelatin cryogel-filled polyurethane nerve guidance channel for neural tissue engineering: fabrication, characterization, and in vitro evaluation. Biomacromolecules 20(2):662–673. https://doi.org/10.1021/acs.biomac.8b01308
123. Rebowe R, Rogers A, Yang X, Kundu SC, Smith TL, Li Z (2018) Nerve repair with nerve conduits: problems, solutions, and future directions. J Hand Microsurg 10(2):61–65. https://doi.org/10.1055/s-0038-1626687
124. Huang L, Zhu L, Shi X, Xia B, Liu Z, Zhu S, Yang Y, Ma T, Cheng P, Luo K (2018) A compound scaffold with uniform longitudinally oriented guidance cues and a porous sheath

promotes peripheral nerve regeneration in vivo. Acta Biomater 68:223–236. https://doi.org/10.1016/j.actbio.2017.12.010
125. Shah MB, Chang W, Zhou G, Glavy JS, Cattabiani TM, Yu X (2019) Novel spiral structured nerve guidance conduits with multichannels and inner longitudinally aligned nanofibers for peripheral nerve regeneration. J Biomed Mater Res B Appl Biomater 107(5):1410–1419. https://doi.org/10.1002/jbm.b.34233
126. Liu J, Saul D, Boker KO, Ernst J, Lehman W, Schilling AF (2018) Current methods for skeletal muscle tissue repair and regeneration. Biomed Res Int 2018:1984879. https://doi.org/10.1155/2018/1984879
127. Kwee BJ, Mooney DJ (2017) Biomaterials for skeletal muscle tissue engineering. Curr Opin Biotech 47:16–22. https://doi.org/10.1016/j.copbio.2017.05.003
128. Abarzua-Illanes PN, Padilla C, Ramos A, Isaacs M, Ramos-Grez J, Olguin HC, Valenzuela LM (2017) Improving myoblast differentiation on electrospun poly(epsilon-caprolactone) scaffolds. J Biomed Mater Res A 105(8):2241–2251. https://doi.org/10.1002/jbm.a.36091
129. Gilbert-Honick J, Iyer SR, Somers SM, Lovering RM, Wagner K, Mao HQ, Grayson WL (2018) Engineering functional and histological regeneration of vascularized skeletal muscle. Biomaterials 164:70–79
130. Gilbert-Honick J, Ginn B, Zhang Y, Salehi S, Wagner KR, Mao HQ, Grayson WL (2018) Adipose-derived stem/stromal cells on electrospun fibrin microfiber bundles enable moderate muscle reconstruction in a volumetric muscle loss model. Cell Transplant 27(11):1644–1656. https://doi.org/10.1177/0963689718805370
131. Yeo M, Kim GH (2018) Anisotropically aligned cell-laden nanofibrous bundle fabricated via cell electrospinning to regenerate skeletal muscle tissue. Small 14(48):1803491
132. Guo Y, Gilbert-Honick J, Somers SM, Mao HQ, Grayson WL (2019) Modified cell-electrospinning for 3D myogenesis of C2C12s in aligned fibrin microfiber bundles. Biochem Biophys Res Commun 516(2):558–564. https://doi.org/10.1016/j.bbrc.2019.06.082
133. Wang L, Wu YB, Guo BL, Ma PX (2015) Nanofiber yarn/hydrogel core–shell scaffolds mimicking native skeletal muscle tissue for guiding 3D myoblast alignment, elongation, and differentiation. ACS Nano 9(9):9167–9179. https://doi.org/10.1021/acsnano.5b03644
134. Yeo M, Lee H, Kim GH (2016) Combining a micro/nano-hierarchical scaffold with cell-printing of myoblasts induces cell alignment and differentiation favorable to skeletal muscle tissue regeneration. Biofabrication 8(3):035021. https://doi.org/10.1088/1758-5090/8/3/035021
135. Yeo M, Kim G (2019) Nano/microscale topographically designed alginate/PCL scaffolds for inducing myoblast alignment and myogenic differentiation. Carbohydr Polym 223:115041. https://doi.org/10.1016/j.carbpol.2019.115041
136. Lee H, Kim W, Lee J, Yoo JJ, Kim GH, Lee SJ (2019) Effect of hierarchical scaffold consisting of aligned dECM nanofibers and poly(lactide-co-glycolide) struts on the orientation and maturation of human muscle progenitor cells. ACS Appl Mater Interfaces 11(43):39449–39458. https://doi.org/10.1021/acsami.9b12639
137. Jana S, Leung M, Chang J, Zhang M (2014) Effect of nano- and micro-scale topological features on alignment of muscle cells and commitment of myogenic differentiation. Biofabrication 6(3):035012. https://doi.org/10.1088/1758-5082/6/3/035012
138. Park J, Choi JH, Kim S, Jang I, Jeong S, Lee JY (2019) Micropatterned conductive hydrogels as multifunctional muscle-mimicking biomaterials: graphene-incorporated hydrogels directly patterned with femtosecond laser ablation. Acta Biomater 97:141–153. https://doi.org/10.1016/j.actbio.2019.07.044
139. Ebrahimi M, Ostrovidov S, Salehi S, Kim SB, Bae H, Khademhosseini A (2018) Enhanced skeletal muscle formation on microfluidic spun gelatin methacryloyl (GelMA) fibres using surface patterning and agrin treatment. J Tissue Eng Regen Med 12(11):2151–2163. https://doi.org/10.1002/term.2738
140. Kim J, Leem J, Kim HN, Kang P, Choi J, Haque MF, Kang D, Nam S (2019) Uniaxially crumpled graphene as a platform for guided myotube formation. Microsyst Nanoeng 5:53. https://doi.org/10.1038/s41378-019-0098-6
141. Suarez AMA, Zhou QH, van Rijn P, Harmsen MC (2019) Directional topography gradients drive optimum alignment and differentiation of human myoblasts. J Tissue Eng Regen Med 13(12):2234–2245. https://doi.org/10.1002/term.2976
142. Grigola MS, Dyck CL, Babacan DS, Joaquin DN, Hsia KJ (2014) Myoblast alignment on 2D wavy patterns: dependence on feature characteristics and cell–cell interaction. Biotechnol Bioeng 111(8):1617–1626. https://doi.org/10.1002/bit.25219
143. Apsite I, Uribe JM, Posada AF, Rosenfeldt S, Salehi S, Ionov L (2019) 4D biofabrication of skeletal muscle microtissues. Biofabrication 12(1):015016. https://doi.org/10.1088/1758-5090/ab4cc4
144. Zabrzynski J, Lapaj L, Paczesny L, Zabrzynska A, Grzanka D (2018) Tendon—function-related structure, simple healing process and mysterious ageing. Folia Morphol 77(3):416–427. https://doi.org/10.5603/FM.a2018.0006
145. Walden G, Liao X, Donell S, Raxworthy MJ, Riley GP, Saeed A (2017) A clinical, biological, and biomaterials perspective into tendon injuries and regeneration. Tissue Eng Part B Res 23(1):44–58. https://doi.org/10.1089/ten.teb.2016.0181
146. Zhang H, Liu MF, Liu RC, Shen WL, Yin Z, Chen X (2018) Physical microenvironment-based inducible scaffold for stem cell differentiation and tendon regeneration. Tissue Eng Part B Rev 24(6):443–453. https://doi.org/10.1089/ten.TEB.2018.0018
147. Lim WL, Liau LL, Ng MH, Chowdhury SR, Law JX (2019) Current progress in tendon and ligament tissue engineering. Tissue Eng Regen Med 16(6):549–571. https://doi.org/10.1007/s13770-019-00196-w
148. Stace ET, Nagra NS, Tiberwel S, Khan W, Carr AJ (2018) The use of electrospun scaffolds in musculoskeletal tissue engineering: a focus on tendon and the rotator cuff. Curr Stem Cell Res Therapy 13(8):619–631
149. Breidenbach AP, Gilday SD, Lalley AL, Dyment NA, Gooch C, Shearn JT, Butler DL (2014) Functional tissue engineering of tendon: establishing biological success criteria for improving tendon repair. J Biomech 47(9):1941–1948. https://doi.org/10.1016/j.jbiomech.2013.10.023
150. Domingues RM, Chiera S, Gershovich P, Motta A, Reis RL, Gomes ME (2016) Enhancing the biomechanical performance of anisotropic nanofibrous scaffolds in tendon tissue engineering: reinforcement with cellulose nanocrystals. Adv Healthc Mater 5(11):1364–1375. https://doi.org/10.1002/adhm.201501048
151. Pauly HM, Kelly DJ, Popat KC, Trujillo NA, Dunne NJ, McCarthy HO, Haut Donahue TL (2016) Mechanical properties and cellular response of novel electrospun nanofibers for ligament tissue engineering: effects of orientation and geometry. J Mech Behav Biomed Mater 61:258–270. https://doi.org/10.1016/j.jmbbm.2016.03.022
152. Wang W, He J, Feng B, Zhang Z, Zhang W, Zhou G, Cao Y, Fu W, Liu W (2016) Aligned nanofibers direct human dermal fibroblasts to tenogenic phenotype in vitro and enhance tendon regeneration in vivo. Nanomedicine (London) 11(9):1055–1072. https://doi.org/10.2217/nnm.16.24
153. Yin Z, Chen X, Song HX, Hu JJ, Tang QM, Zhu T, Shen WL, Chen JL, Liu H, Heng BC, Ouyang HW (2015) Electrospun scaffolds for multiple tissues regeneration in vivo through topography dependent induction of lineage specific differentiation. Biomaterials 44:173–185. https://doi.org/10.1016/j.biomaterials.2014.12.027

154. Orr SB, Chainani A, Hippensteel KJ, Kishan A, Gilchrist C, Garrigues NW, Ruch DS, Guilak F, Little D (2015) Aligned multilayered electrospun scaffolds for rotator cuff tendon tissue engineering. Acta Biomater 24:117–126. https://doi.org/10.1016/j.actbio.2015.06.010
155. Wu S, Wang Y, Streubel PN, Duan B (2017) Living nanofiber yarn-based woven biotextiles for tendon tissue engineering using cell tri-culture and mechanical stimulation. Acta Biomater 62:102–115. https://doi.org/10.1016/j.actbio.2017.08.043
156. Xu Y, Wu J, Wang H, Li H, Di N, Song L, Li S, Li D, Xiang Y, Liu W, Mo X, Zhou Q (2013) Fabrication of electrospun poly(L-lactide-co-epsilon-caprolactone)/collagen nanoyarn network as a novel, three-dimensional, macroporous, aligned scaffold for tendon tissue engineering. Tissue Eng Part C Methods 19(12):925–936. https://doi.org/10.1089/ten.TEC.2012.0328
157. Yang C, Deng G, Chen W, Ye X, Mo X (2014) A novel electrospun-aligned nanoyarn-reinforced nanofibrous scaffold for tendon tissue engineering. Colloids Surf B Biointerfaces 122:270–276. https://doi.org/10.1016/j.colsurfb.2014.06.061
158. Lenzi TL, Guglielmi Cde A, Arana-Chavez VE, Raggio DP (2013) Tubule density and diameter in coronal dentin from primary and permanent human teeth. Microsc Microanal 19(6):1445–1449. https://doi.org/10.1017/S1431927613012725